Desalination 602 (2025) 118570

Contents lists available at ScienceDirect

Desalination

journal homepage: www.elsevier.com/locate/desal

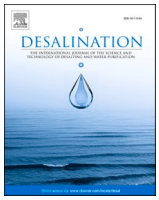

Factors affecting the efficiency of electrochemical lithium extraction: A systematic review from materials to processes technology

Junyi Zhang [a,1], Tiandong Chen [a,1], Luxiang Ma [a,*], Chunxi Hai [a], Yanxia Sun [a], Shengde Dong [a], Xin He [a], Qi Xu [a], Jitao Chen [c], Hongli Su [b,*], Yuan Zhou [a,*]

[a] College of Materials and Chemistry & Chemical Engineering, Cheng Du University of Technology, Cheng Du 610059, PR China
[b] Resource Recycling, Department of Engineering Structures, Faculty of Civil Engineering and Geosciences, Delft University of Technology, Delft, 2628, CN, the Netherlands
[c] College of Chemistry and Molecular Engineering, Peking University, Beijing, 100871, PR China

HIGHLIGHTS

- The influence of lithium extraction efficiency from material to process parameters was evaluated.
- The challenges of electrochemical lithium extraction technology are prospected.
- It provides a more comprehensive reference for the truly efficient industrialization of electrochemical lithium extraction.

GRAPHICAL ABSTRACT

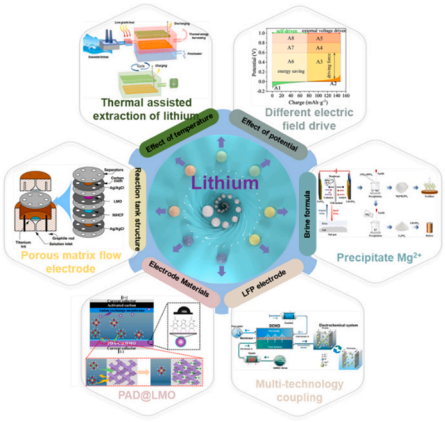

ARTICLE INFO

Keywords:
Electrochemical method
lithium extraction from salt lakes
Material modification
Electrolytic cell
Processes technology

ABSTRACT

Electrochemical extraction of lithium (ELE), as a green lithium extraction technology, is of great significance to the exploitation of lithium resources in salt lakes and the sustainable development of the new energy industry. However, the low efficiency and competition of impurity ions limit its large-scale application. In this paper, the current research progress is reviewed from the viewpoint of reaction tank design, electrode material modification, reaction tank process parameter optimization and multi-technology coupling. Additionally, through in-depth research and exploration of these key issues, it is expected to improve the efficiency of electrochemical lithium extraction, reduce energy costs, and promote the practical application and popularization of lithium extraction technology in salt lakes. Finally, this paper discussed the existing challenges and outlooks to improve the performance of ELE, meeting the rising global demand for lithium sources.

* Corresponding authors.
E-mail addresses: maluxiang@cdut.edu.cn (L. Ma), suhong@deakin.edu.au (H. Su), zhouy@cdut.edu.cn (Y. Zhou).
[1] Junyi Zhang and Tiandong Chen have same contribution to the publication.

https://doi.org/10.1016/j.desal.2025.118570
Received 4 July 2024; Received in revised form 3 January 2025; Accepted 13 January 2025
Available online 22 January 2025
0011-9164/

1. Introduction

The global surge in demand for clean energy has propelled rapid development in energy storage, new energy vehicles, and associated industries [1]. Lithium-ion batteries, serving as pivotal energy storage devices for new energy vehicles, have emerged as the predominant battery technology owing to their high energy density, long lifespan, and eco-friendliness [2]. Nevertheless, the demand for lithium resources escalates daily as the new energy vehicle market expands (Fig. 1a), while traditional lithium resource reservoirs encounter progressively constrictive constraints [3,4]. Consequently, the requirements for novel lithium resource reservoirs have emerged as a prominent area of contemporary research. Salt lake brine is widely recognized as a potential sustainable lithium resource reserve. Over 60 % of the world's lithium resources exist in salt lake brine (Fig. 1b) [5]. Thus, it is vital to extract Li^+ from salt lakes to meet the demand for the new energy industry [5,6]. Currently, evaporation technologies used to extract lithium from brine rely on open air evaporation to concentrate brine. In this process, Depending on the deposit, a large amount of water, approximately 100–800 cubic meters per tonne of lithium carbonate, is lost during the evaporation process [7]. Additionally, natural evaporation is relatively slow, typically taking 10 to 24 months, and is influenced by climatic conditions. Furthermore, the process demands high brine quality, which further constrains its effectiveness. Consequently, there is an urgent need to explore economically viable technologies for developing thinner lithium resources to diversify lithium production. These technologies are primarily categorized into two processes (Fig. S1): Direct Lithium Extraction (DLE) and Lithium Brine Concentration (LBC). The DLE process focuses on the selective extraction of lithium from saltwater, leading to the production of a final lithium product in subsequent stages. In contrast, the LBC process concentrates lithium brine without separating lithium from it, aims to remove impurities, and produces the final lithium product later. Thus, while the LBC process shares a similar goal with evaporation ponds, it efficiently recovers water, mitigating losses [8].

Among the DLE and LBC of techniques, electrochemical Lithium Extraction (ELE) has emerged as a prominent research area for Li^+ extraction from salt lakes, owing to its relatively environmental

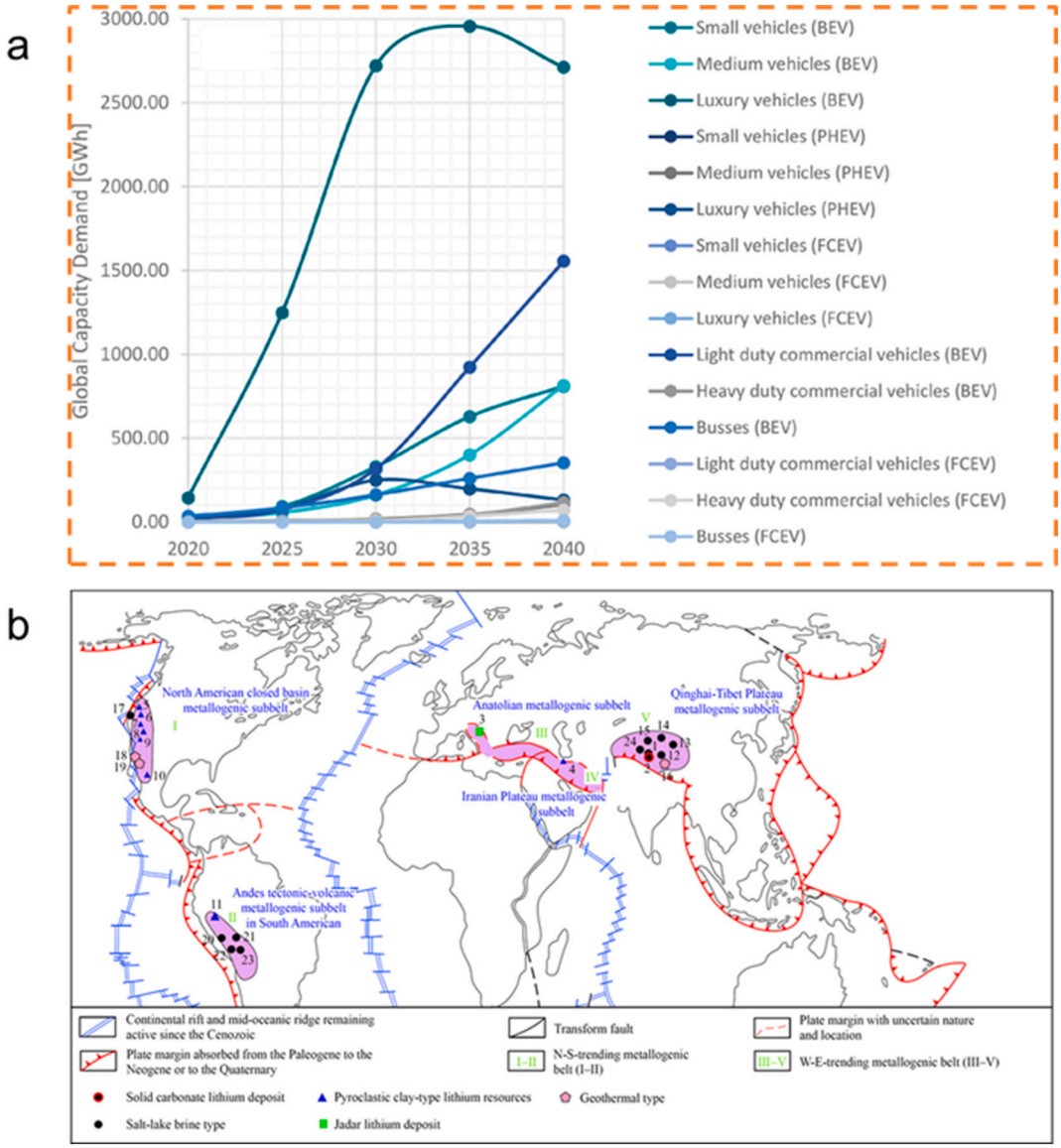

Fig. 1. Lithium demand and distribution map. (a) Estimation of the global capacity demand of EVs in 2040. Reprinted with permission [3], copyright 2023, Elsevier. (b) Schematic diagram showing the zonation and distributions of global Cenozoic exogenetic lithium resources. Reprinted with permission [5], copyright 2023, Elsevier.

friendliness and streamlined process [9,10]. This method can selectively and efficiently extract Li^+ from salt lake brine via electrochemical reactions under appropriate potential conditions [11,12]. Despite significant advancements, ELE encounters various challenges, including low Li^+ extraction efficiency, competition from impurity ions, and high energy costs [13,14]. Comprehensive research is imperative to address these issues and foster the utilization of ELE from salt lakes. The aims are to improve ELE efficiency, achieve optimal selective extraction, reduce energy costs, further promote the development of electrochemical lithium extraction from salt lakes, and significantly contribute to the sustainable development of the clean energy industry.

2. Factors impacting the performance of ELE

Kanoh et al. (1993) first reported the ELE method [15]. Then, various electrochemical methods have been studied to recover Li^+ from liquid resources, including electrochemical switched ion exchange (ESIX) [16,17], capacitive deionization/electrochemical adsorption (CDI) [18,19], current electrode capacitive deionization (FCDI) [20,21], electrodialysis (ED) [21,22], and electrochemical desalination (EDM) [11,23].Most ELE systems are similarly with water-based lithium-ion batteries, primarily through Reduction-Oxidation (REDOX) reactions of the positive electrode material when energized, facilitating Li^+ intercalation. Among these methods, ED stands out as it employs an electric field to selectively drive ions through the exchange membrane, thereby achieving ion separation and enrichment. Fig. 2 outlines the principles and development history of Li^+ extraction using various ELE technologies [17,24–26]. These systems significantly affect Li^+ extraction efficiency, encompassing material properties, process parameters, and technology integration. This paper will review the following topics: (1) modification and development of electrode materials, (2) optimization of reaction tank design and investigation of kinetic properties, (3) pretreatment strategies for salt lake brine, and (4) the integration of electrochemistry with complementary technologies. The article primarily summarizes current research solutions addressing these key scientific challenges, while also highlighting existing issues and providing insights into future developments.

2.1. Modification of electrode materials and development of new electrode materials

Lithium extraction efficiency encompasses both the kinetics of Li^+ extraction and the Li^+ recovery capacity per unit area. The structure and performance of electrode materials directly influence Li^+ extraction efficiency. Based on the relationship between the voltage of electrode materials in an aqueous solution and pH (ϕ-pH diagram) (Fig. 3a) [27], electrode materials that can stably exist in an aqueous solution (e.g., lithium vanadate (LiV_3O_8), lithium iron phosphate ($LiFePO_4$/LFP), spinel lithium manganate ($LiMn_2O_4$/LMO), lithium nickelate ($LiNiO_2$), activated carbon (AC), and vanadium oxide (VO_2)). It is evident that olivine-like LFP (Fig. 3b) and spinel-like LMO (Fig. 3c) are more suitable for ELE by comparing the structure, cost, environmental impact, and performance (Table 1) [28]. The LMO electrodes demonstrate excellent performance akin to that of spinel λ-MnO_2 ion screens regarding Li^+ adsorption capacity and selectivity [29]. LMO materials are more environmentally friendly and efficient in electrochemical halogenation of Li^+ extraction compared to the time-consuming and pickling process of manganese ion screen adsorbents. However, LMO is prone to disproportionation of Mn^{3+}, resulting in Mn dissolution loss, resulting in structural collapse, limiting its widespread use in ELE [30]. In addition, the LFP electrode is susceptible to impurity elements like Mg^{2+} in salt lake brine, which reduces its selectivity, thereby constraining its

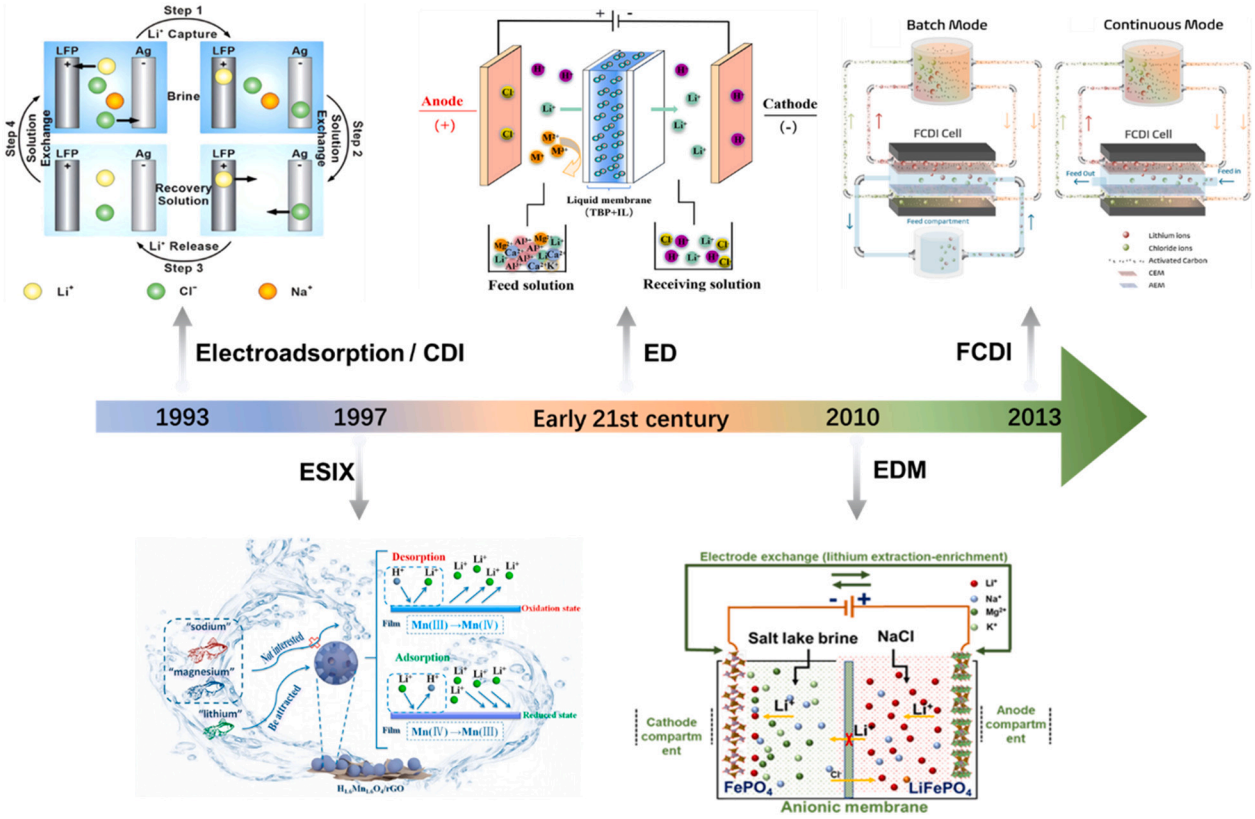

Fig. 2. From left to right are the principle of electroadsorption /CDI. Reprinted with permission [24], copyright 2018, Royal Society of Chemistry. The principle of ESIX. Reprinted with permission [17], copyright 2019, Elsevier. The principle of ED. Reprinted with permission [25], copyright 2024, Elsevier. The principle of electrochemical de-lithiation method and the principle of FCDI. Reprinted with permission [26], copyright 2019, MDPI.

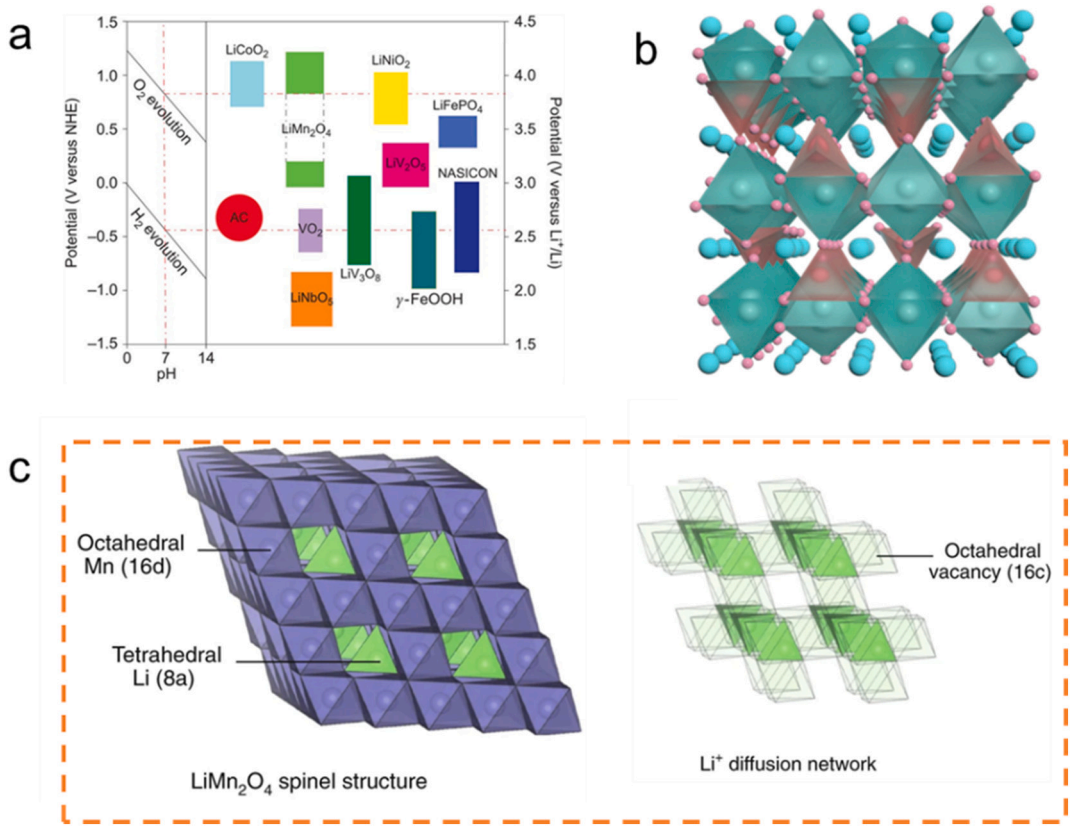

Fig. 3. Electrode material structure and ϕ-pH diagram. (a) ϕ-pH diagram of electrode material in water. Reprinted with permission [27], copyright 2010, Nature Publishing Group. Crystal structure of LFP (b) and LMO (c). Reprinted with permission [31], copyright 2020, Nature Publishing Group.

industrial application in brines with high magnesia-lithium ratios. Consequently, This section mainly reviews and summarizes the related strategies implemented for defects of LMO and LFP materials.

2.1.1. Spinel structure LMO

As an electrode material, spinel LMO has widely applied for Li^+ extraction from brines. The mechanism of Li^+ de-intercalation in LMO has been deeply researched and three main mechanisms are suggested, including (1) ion exchange; (2) compound mechanism; and (3) REDOX [32]. Ion exchange typically involves the use of an acid to facilitate the exchange of Li^+ for H^+, thereby leaving the positions of Mn^{3+} and Mn^{4+} within the LMO crystal unchanged while replacing solid Li + with protons. This compound mechanism encompasses the coupling of ion exchange and redox reactions. However, in the ELE process, no acid is utilized, yet electron transfer still occurs. Consequently, the redox mechanism effectively elucidates the de-intercalation process of LMO during ELE, incorporating models such as the surface disproportionation model, stage model, and adsorption model. Hunter et al. [33] introduced a surface disproportionation model in 1981. Briefly, Mn^{3+} on the surface of LMO undergoes disproportionation, generating Mn^{2+} and Mn^{4+}. Simultaneously, with the dissolution of Mn^{2+}, surface Mn^{4+} and internal Mn^{3+} transform. Li^+ diffuses from the interior of LMO to its surface as a free ion, ultimately dissolving into the solution (Eq. (1)).

$$4Li\left[Mn^{4+}, Mn^{3+}\right]O_4 + 8H^+ = 3(\circ)\left[Mn_2^{4+}\right]O_4 + 4Li^+ + 2Mn^{2+} + 4H_2O \quad (1)$$

Where ∘ represents the hole position within the spinel structure. Ooi et al. [34] employed a phase model for the intercalation of λ-MnO_2 in Li^+ in aqueous solution. The Li^+ intercalation process can be divided into two steps: (1) Li^+ intercalation into the vacant tetrahedral site of the λ-MnO_2 framework (Eq. (2)), accompanied by the reduction from Mn^{4+} to Mn^{3+}; (2) migration of excess electrons (xe-) to the surface of λ-MnO_2 and oxidation of hydroxyl ions in the aqueous phase (Eq. (3))

$$\lambda - MnO_2 + xLi^+ + xe^- = Li_xMnO_2 \quad (2)$$

$$xOH^- = \left(\frac{x}{2}\right)H_2O + \left(\frac{x}{4}\right)O_2 + xe^- \quad (3)$$

Marchini et al. [35] reported an adsorption model for Li^+ intercalation, involving partial de-solvation of ions in a solution near the intercalated electrode and subsequent adsorption of ions on the electrode surface. It considers the loss of bound water during Li^+ de-solvation as it diffuses to LMO surface. Moreover, as Mn^{4+} gains electrons, Li^+ is further inserted into the tetrahedral sublattice of the spinel structure [35]. The diffusion of Li^+ and the electrode adsorption process are accompanied by phase transitions between the intercalation stages.

When Mn^{3+} undergoes disproportionation in LMO, the spinel crystal structure is altered or even destroyed, disrupting the three-dimensional (3D) ion migration channels crucial for Li^+ transport and hindering their reversible intercalation. To address this issue, macrostructures such as porous materials and nanorods have been designed and fabricated to enhance the specific surface area [36,37]. This design approach increases the number of active sites, thereby facilitating Li^+ transmission. Additionally, interfacial modification or site doping can effectively mitigate the Jahn-Teller distortion of Mn, thereby improving cycle stability [38,39]. Increasing the active sites and porous channels of LMO can effectively enhance ion transport kinetics and charge transfer in micropores. Chao et al. [40] designed a porous disk-like LMO using a weak cationic surfactant, polyethylpyrrolidone (PVP), which has both hydrophilic and lipophilic properties that regulate morphology during the reaction (Fig. 4a). PVP's oleophilic group adsorbs manganese acetylacetone, forming porous disk-like materials. This increases the material's specific surface area, enhancing the exchange with Li^+. Additionally, Gu et al. [41] designed octahedral LMO with controllable

Table 1
The advantages and shortcomings of key materials [28].

Materials	Structure	Advantage	Shortcoming
LMO	Spinel structure *Fd3m* space group	High Li^+ adsorption capacity. High Li^+ selectivity. Wide sources of raw materials. Low cost. Environmentally friendly. Simple preparation. Excellent low-temperature performance.	pH sensitivity. Jahn-Teller effect leads to LMO structure collapse. In complete water decomposition
LFP	Orthogonal olivine structure Pnma space group	High selectivity. Low cost. Ecofriendly. Good chemical stability at high temperatures and pressures. Reversible property. Medium operating voltage. High specific capacity	Small vibration density. Large size. Poor electrical conductivity. Slow Li^+ diffusion. Poor performance at low temperatures.
Li[NiMn]O_2 (LNMO)	Cubic spinel structure *Fd3m* space group	Excellent stability and selectivity (>1000 cycles). Low energy consumption. High purity of Li^+ extraction. Fast Li + extraction due to tetrahedral diffusion. Inhibits oxygen evolution.	Small presence of secondary phases. Low theoretical specific capacity (147 $mAh{\cdot}g^{-1}$).
Li[NiCoMn]O_2 (LNCM)	Layered hexagonal α-$NaFeO_2$ structure *R3m* space group	High theoretical capacity (275 $mAh{\cdot}g^{-1}$). Minimal volume change at 2.5–4.4 V. Fast and reliable charge discharge characteristics. Strong stability	High operating costs due to energy consumption. Rigorous preparation. Poor thermal stability.
$Li_3V_2(PO_4)_3$	Monoclinic structure *P21/n* space group	Abundant synthetic raw materials, low production cost, good cycle performance, structural stability	Poor electronic conductivity and slow lithium ion diffusion rate.
LiV_3O_8	Monoclinic structure *P21/m* space group	Good structural stability, low cost, good safety.	Low conductivity, strong oxidation

particle size by adjusting the water-to-ethanol ratio in the precursor solution (Fig. 4b). Electrochemical performance tests indicate that as particle size increases, LMO's cyclic stability and Li^+ transport performance improve. The Mn dissolution loss per 30 cycles of LMO was 0.187 %, with the volume remaining at 86.9 % of the initial value.

Lithium manganese oxide (LMO) materials are thermodynamically unstable and prone to the disproportionation of Mn^{3+}, which leads to the Jahn-Teller effect and manganese leaching. To mitigate these issues, surface modification or coating is commonly employed to enhance stability and reduce leaching [42]. Wang et al. [43] used dopamine hydrochloride (PAD) to modify the surface of the $Li_{1.6}Mn_{1.6}O_4$ electrode. PAD, rich in carboxyl and amino groups, improved the material's hydrophilicity, mitigated Mn disproportionation, and reduced Mn dissolution loss. The Li^+ extraction capacity of the coated electrode increased from 20.0 $mg{\cdot}g^{-1}$ to 39.6 $mg{\cdot}g^{-1}$ (Fig. 5a). Meanwhile, Luo et al. [44] prepared CeO_2@LMO by the sol-gel method, achieving a capacity retention rate of 60 % and an Mn dissolution loss rate of 0.016 % after 30 cycles at 50 mA (Fig. 5b). CeO_2 inhibits the agglomeration of active metal oxides, promoting contact and electron transfer. Additionally, Gu et al. [45] improved hydrophilicity by depositing amorphous $AlPO_4$ on the LMO surface, achieving a capacity retention rate of 93.6 % after 20 cycles, with an Mn dissolution loss of only 0.147 % (Fig. 5c). Hao et al. [46] prepared a 3D porous λ-MnO_2/rGO/Naalg hybrid membrane, constructing a 3D conductive network to enhance the material's kinetic properties. The composite membrane's adsorption capacity reached 32.7 $mg{\cdot}g^{-1}$, with equilibrium adsorption over 90 % within 1 h. Furthermore, Mu et al. [47] used 3D graphite felt to load LMO. The mesoporous LMO composite with a large specific surface area of 183 $m^2{\cdot}g^{-1}$ had a wide solid-liquid interface for Li^+ intercalation and an excellent Li^+ extraction kinetics of 75 $mg{\cdot}h^{-1}$.

Additionally, LMO strucutres can be effectively stabilized by doping LMO with cations of lower activity elements. For example, Tian et al. [48] doped the transition metal - Cr on LMO to inhibit Mn disproportionation, reducing the Mn dissolution with a rate of 0.027 % per cycle (Fig. 5d). After 500 cycles, the Li^+ extraction amount reached 22 $mg{\cdot}g^{-1}$ with a retention rate of 86.05 %. Furthermore, Meng et al. [49] prepared a $LiNi_{0.05}Mn_{1.95}O_4$ (LNMO_0.05) electrode material with truncated octahedron characteristics through Ni doping and crystal plane structure control. This material leverages the high Li^+ diffusion properties of the (100) crystal plane and the stability of the (111) crystal plane to enhance

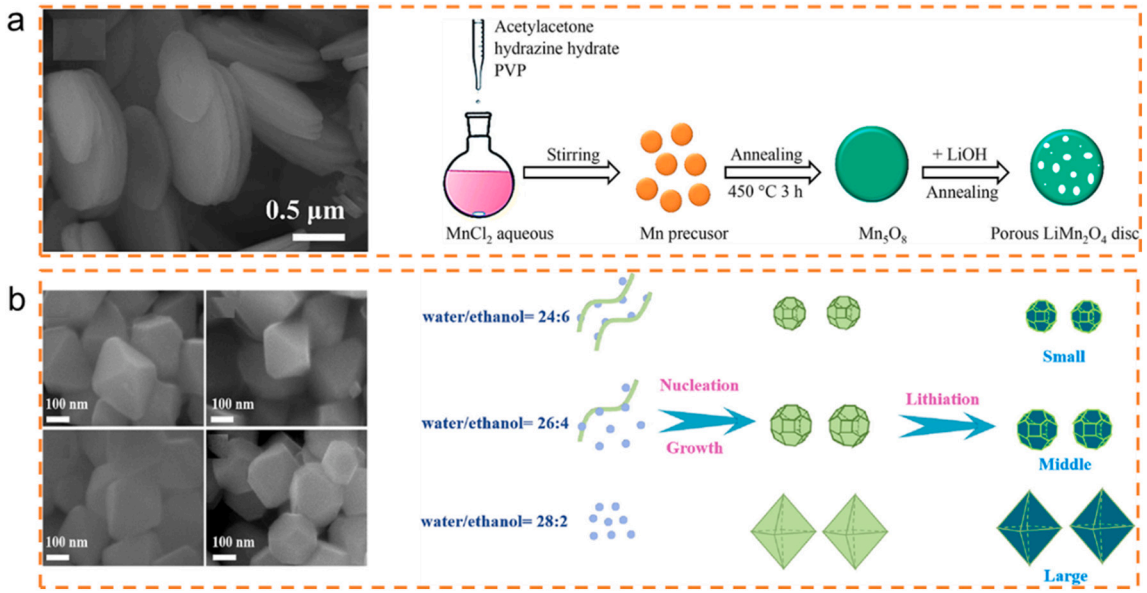

Fig. 4. Modification of LMO. (a) SEM image of Mn5O8 and formation flow chart of porous disc LMO. Reprinted with permission [40], copyright 2023, Elsevier. (b) Synthesis roadmap and SEM images of LMO with different particle sizes. Reprinted with permission [41], copyright 2023, Elsevier.

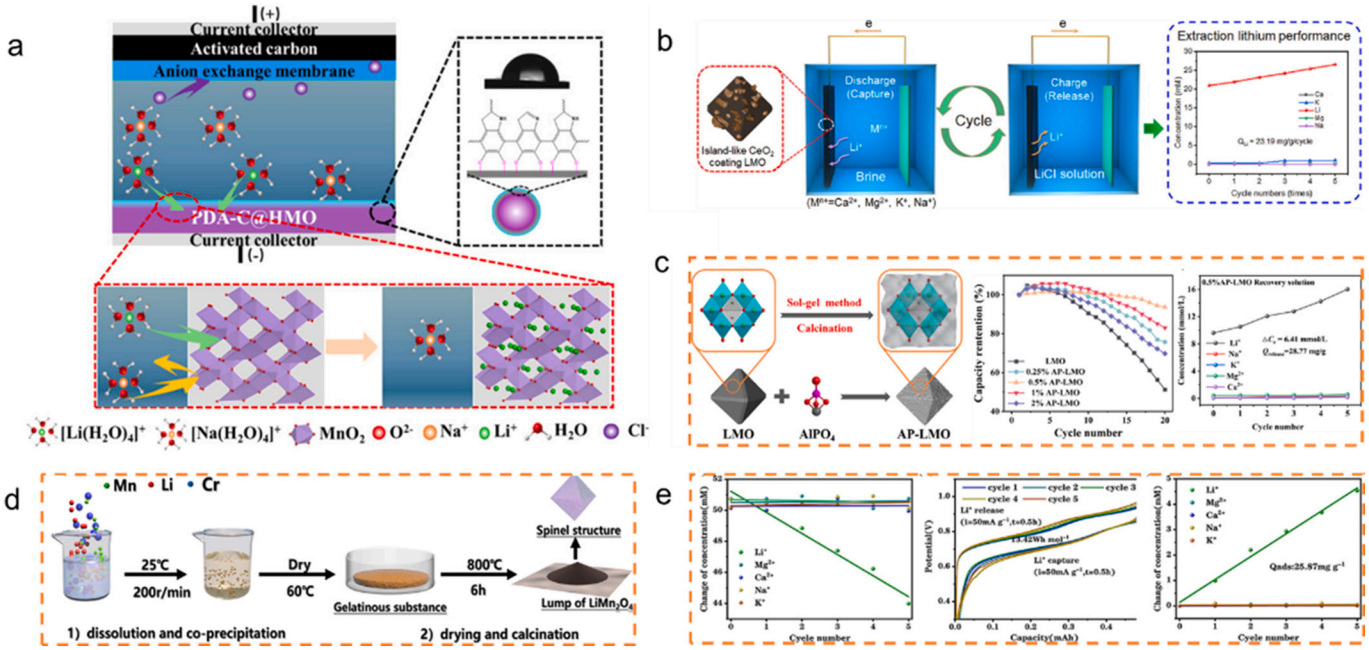

Fig. 5. Modification of LMO. (a) PDA-C@HMO electrode adsorption coupling electrochemical extraction of lithium schematic diagram.Reprinted with permission [43], copyright 2022, American Chemical Society. (b) Schematic diagram of ELE of Ce-LMO-2|Ag electrochemical system and adsorption capacity of each ion under five cycles. Reprinted with permission [44], copyright 2023, Elsevier. (c) AP-LMO electrode material synthesis and Li^+ extraction performance. Reprinted with permission [45], copyright 2023, Elsevier. (d) The flow chart of chrome-doped spinel type LMO was synthesized by precipitation calcination method. Reprinted with permission [48], copyright 2024, Elsevier; (e) LNMO-0.05 electrode electrochemical Li^+ extraction cycle performance and average energy consumption curve. Reprinted with permission [49], copyright 2024, Elsevier.

Li^+ extraction performance. Experimental results show that the cyclic properties and diffusion coefficients of this doped material are superior to undoped LMO electrodes (Fig. 5e). These doping strategies combine the advantages of surface coatings with high adsorption capacity, enhanced transport capabilities, and improved cathode stability.

Most researchers have used strategies such as element doping, surface coating, structural regulation, and conductive material composites to enhance the Li^+ extraction performance [40,46,50,51]. Elemental doping improves structural stability by replacing Mn^{3+} in the octahedron with cations of similar atomic size and valency. Surface coating with protective materials reduces direct contact between the electrode material and brine, inhibiting Mn disproportionation. This approach uses inorganic materials like precious metals and metal oxides to effectively enhances LMO's electrical conductivity, cycle stability, and electrochemical activity. Organic materials have good film-forming properties and uniform coating, which reduces Mn^{3+} dissolution and promotes Li^+ transport. Structural regulation increases the specific surface area, shortens ion transport distances, and exposes adsorption active sites, thereby improving adsorption capacity and cycle stability. The composite strategy utilizes the superior electronic conductivity of carbon-based materials to improve the electrical conductivity of LMO, accelerate electron transfer rates, and enhance its electrochemical activity.

2.1.2. Olivine LFP

LFP has an orthorhombic olivine structure and belongs to the Pnma space group. The migration of Li^+ in LFP mainly occurs along the direction of the hexagonal close-packed arrangement of oxygen. During Li^+ removal, a REDOX reaction of Fe^{2+}/Fe^{3+} occurs (as shown in) Eqs. (4) and (5)). Within the unit cell, the PO_4 tetrahedron is established between P and O. The high bond energy of the P–O covalent bond enhances the stability and safety of the battery during charge and discharge cycles, while simultaneously mitigating the risk of O_2 generation. Lithium and iron form octahedra, specifically LiO_6 and FeO_6, coordinated by surrounding oxygen atoms. The adjacent FeO_6 octahedra share a common vertex, resulting in a less cohesive arrangement of iron atoms, which in turn leads to diminished electrical conductivity. During charge and discharge, the transport of Li^+ is affected by the presence of FeO_6 and PO_4, necessitating a wavy diffusion path that reduces Li^+ diffusion efficiency.

$$LiFe^{II}PO_{4-x}Li^+ - xe^- \rightarrow xFe^{III}PO_4 + (1-x)LiFe^{II}PO_4 \quad (4)$$

$$Fe^{III}PO_4 + yLi^+ + ye \rightarrow yLLiFe^{II}PO_4 + (1-y)Fe^{III}PO_4 \quad (5)$$

The diffusion mechanism of Li^+ is a focus of research. Li^+ diffuses one-dimensionally (1D) along the B-axis in LFP, resulting in lower Li^+ extraction kinetics during the electrochemical process [52]. This is typically improved by coating fast ion electronic conductors and controlling the growth of Li^+ diffusion surfaces.

Wang et al. [53] used phytic acid (PhyA) as a phosphorus source, an internal carbon source, and an antioxidant to synthesize a lithium ferrous phosphate precursor (IC/LFP) containing internal carbon through a solvothermal method. The precursor was then mixed with glucose (GC) to obtain GC-coated LFP and subsequently calcined to create a composite material (GC/IC/ILFP). In the artificial salt lake brine, at an applied potential of 0.8 V, the intercalation Li^+ capacity reached 38.09 $mg{\cdot}g^{-1}$, which is 86.57 % of the theoretical capacity. The outgoing capacity was 35.00 $mg{\cdot}g^{-1}$ and 91.89 % of the intercalation capacity. The rich carbon content improves conductivity, but it may inhibit Li^+ diffusion and increase the ion diffusion path. For example, Zhang et al. [54] dispersed LFP uniformly in a carbon matrix through in-situ polymerization of resorcinol and formaldehyde from lithium, iron, and phosphorus sources at high temperatures. The carbon materials form a 3D skeleton of interconnected carbon spheres, where LFP grows in situ. This unique 3D carbon mesh hierarchical porous structure (Fig. 6a) achieved an intercalation capacity of 5.13 $mg{\cdot}cm^{-3}$, nearly twice that of electrodes prepared by traditional methods. Jin et al. [55] reported modification of LFP with carbon coating and hydrophilic polydopamine (pD) coating (Fig. 6b) to improve conductivity and wettability. This increases the ion concentration and mobility around the

electrode, providing more energy for Li^+ and overcoming the intercalation energy barrier. Wang et al. [53] used phytic acid (PhyA) as a phosphorus source, an internal carbon source, and an antioxidant to synthesize a lithium ferrous phosphate precursor (IC/LFP) containing internal carbon through a solvothermal method. The precursor was then mixed with glucose (GC) to obtain GC-coated LFP and subsequently calcined to create a composite material (GC/IC/ILFP). In the artificial salt lake brine, at an applied potential of 0.8 V, the intercalation Li^+ capacity reached 38.09 $mg{\cdot}g^{-1}$, which is 86.57 % of the theoretical capacity. The outgoing capacity wasThe outgoing capacity was determined to be 35.00 $mg{\cdot}g^{-1}$, which corresponds to 91.89 of the intercalation capacity. Although the elevated carbon content improves conductivity, it may also hinder Li^+ diffusion and increase the length of the ion diffusion pathway.For example, Zhang et al. [54] dispersed LFP uniformly in a carbon matrix through in-situ polymerization of resorcinol and formaldehyde from lithium, iron, and phosphorus sources at high temperatures. The carbon materials form a 3D skeleton of interconnected carbon spheres, where LFP grows in situ. This unique 3D carbon mesh hierarchical porous structure (Fig. 6a) achieved an intercalation capacity of 5.13 $mg{\cdot}cm^{-3}$, nearly twice that of electrodes prepared by traditional methods. Jin et al. [55] reported modification of LFP with carbon coating and hydrophilic polydopamine (pD) coating (Fig. 6b) to improve conductivity and wettability. This increases the ion concentration and mobility around the electrode, providing more energy for Li^+ and overcoming the intercalation energy barrier.

Chen et al. [56] used hydrothermal synthesis to create LFP samples with (100) and (010) exposed crystal faces to explore ion transport behavior (Fig. 6c). Their study demonstrated the effects of exposed crystal faces on ion surface adsorption and volume phase diffusion. This research enhances understanding of the interfacial interaction between Li^+ and LFP at the microscopic level and aids in designing LFP with improved Li^+ extraction kinetics by optimizing its exposure to Li^+ diffusion surfaces. Furthermore, the synthesis of olivine-type FP materials remains a prominent area of research. The preparation process for olivine-type FP cathode materials is intricate, whereas LFP has well-established synthesis methods. Conventional approaches, such as calcination or hydrothermal techniques, often produce FP materials that lack sufficient Li^+ migration channels. As a result, electrochemical methods are typically utilized to prepare FP electrode materials by extracting Li^+ from LFP. Nonetheless, in practical industrial applications, the electrochemical preparation of FP electrodes faces significant challenges, including prolonged processing times and low efficiency, usually requiring 10 to 12 h. To overcome these challenges,Xiong et al. [57] immersed LFP electrodes in a sodium persulfate solution and performed

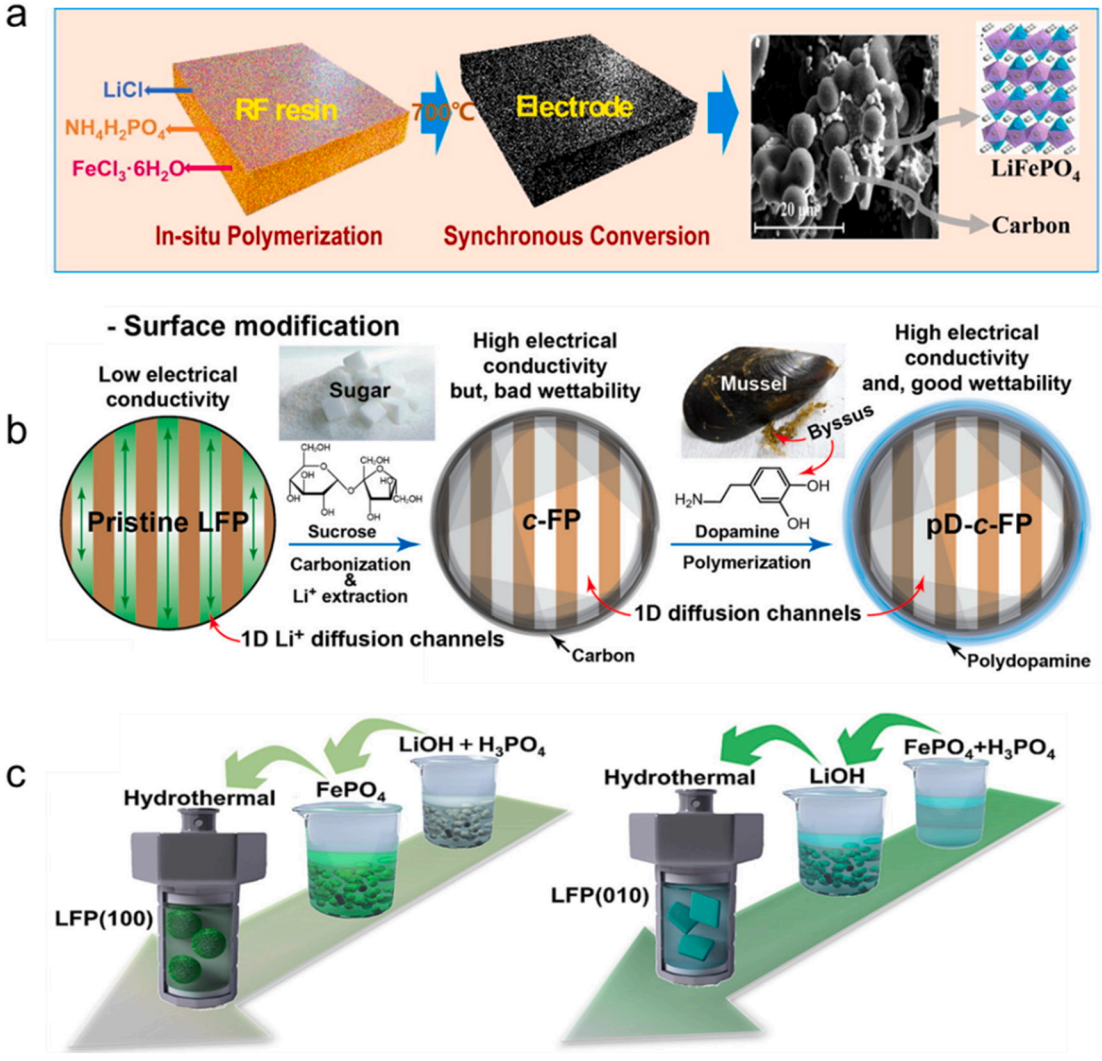

Fig. 6. Modification of LFP. (a) Preparation diagram of porous carbon-supported $LiFePO_4$. Reprinted with permission [54], copyright 2023, Elsevier. (b) Surface modification of LFP and FP. Synthesized pristine LFP (left), carbon-coated FP (c-FP, middle), and polydopamine (pD)-coated c-FP (pD-c-FP, right). Reprinted with permission [55], copyright 2015, American Chemical Society. (c) Synthetic route diagram of LFP(100) and LFP(010). Reprinted with permission [56], copyright 2023, Elsevier.

a chemical oxidation reaction at a specific temperature and time. This method for preparing FP electrodes is simple, efficient, suitable for industrial applications, and offers a new perspective on $FePO_4$ electrode material preparation.

2.1.3. Other materials

ELE also uses LNMO, LNCM, and $Li_3V_2(PO_4)_3$. LNMO powders have a cubic spinel structure belonging to the Fd3m space group, similar to LMO. Mn^{3+} is prone to disproportionation reactions, leading to Mn dissolution. Doping with low-cost metal ions reduces the relative Mn content, thereby decreasing the dissolution likelihood [58]. Zhao et al. [59] successfully prepared $LiNi_{0.03}Mo_{0.01}Mn_{1.96}O_4$ with a good lattice structure using the co-precipitation method. This material extracted up to 14.4 $mg{\cdot}g^{-1}$ of Li^+ in the artificial brine per cycle, with a capacity retention rate of 90.8 % after 30 cycles, showing good stability.

LNCM has a layered hexagonal α-$NaFeO_2$ structure with an R-3 m space group. In this structure, Li and transition metals (Ni, Co, and Mn) occupy sites 3a, 3b, and 6c, respectively [60]. The valence states of Ni and Co change to maintain charge balance during Li^+ de-intercalation in LNCM materials. LNCM exhibits uniform distribution of Ni, Co, and Mn, low cation mixing rates, and good crystal order. For instance, Lawagon et al. [61] used $Li_{(1-x)}Ni_{(1/3)}Co_{(1/3)}Mn_{(1/3)}O_2$ as a lithium-ion intercalation electrode (Fig. 7a) and found that the material had a high Li^+ intercalation capacity. This material exploits the high Li^+ diffusion characteristics of the (100) crystal plane, in conjunction with the stability of the (111) crystal plane, to enhance the performance of Li^+ extraction. Experimental results indicate that both the cyclic performance and diffusion coefficient of this structured material surpass those of undoped LMO electrodes. Meanwhile, Wu et al. [62] prepared $LiNi_{0.025}Co_{0.025}Mn_{1.95}O_4$ powder to form a working electrode. The results show that Ni and Co doping can inhibit the reduction of Mn^{3+} and increase the Li^+ diffusion coefficient. After 15 cycles of Li^+

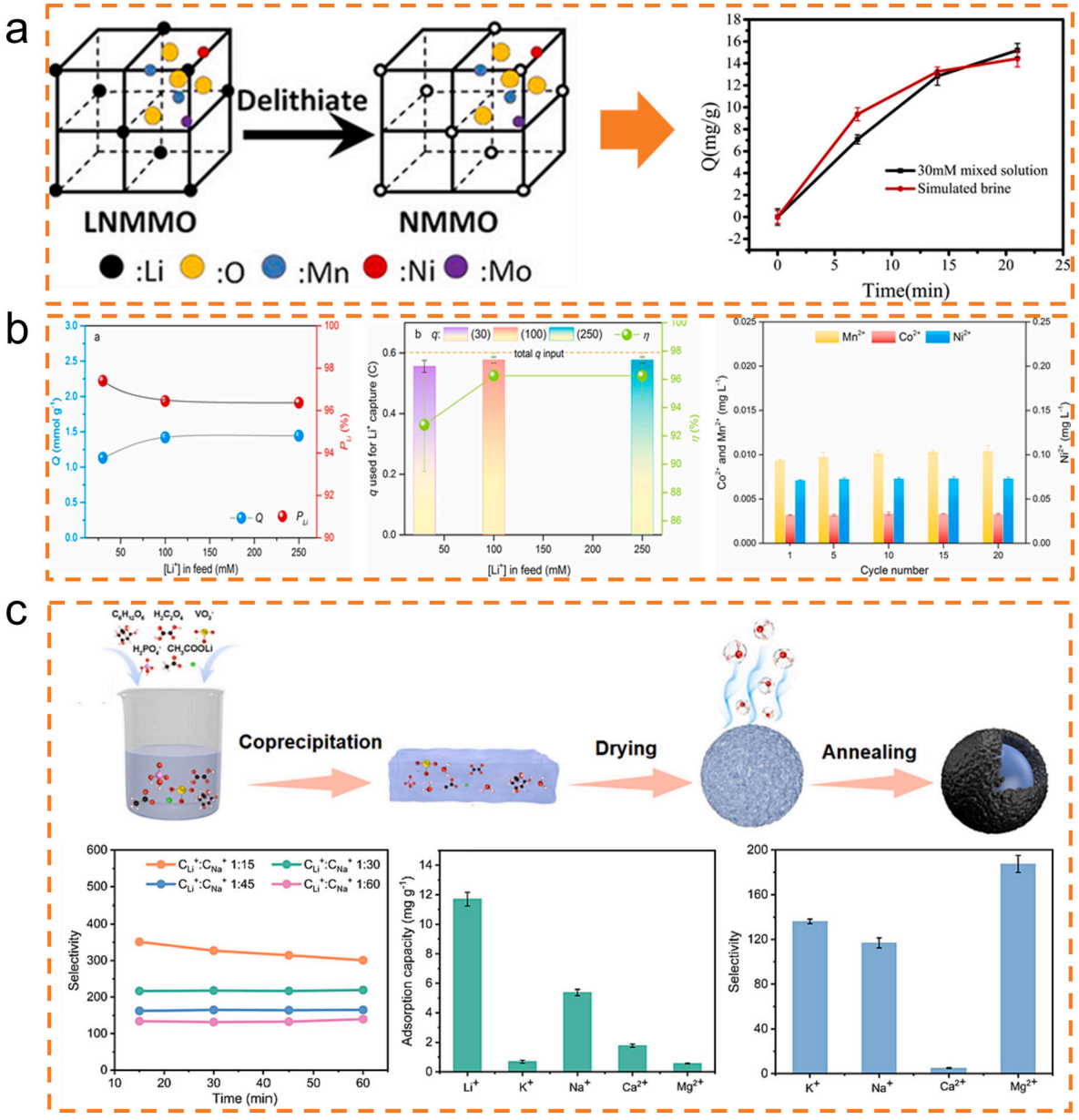

Fig. 7. Other material modification measures. (a) Structural diagram of LNMMO and its lithium extraction performance. Reprinted with permission [61], copyright 2019, Elsevier. (b) Li^+ extraction performance and current efficiency of NCM/Ag system at different concentrations. Reprinted with permission [62], copyright 2023, American Chemical Society. (c) LVP@C schematic diagram of the synthesis process and selectivity of the electrode material for each ion. Reprinted with permission [63], copyright 2024, Elsevier.

deintercalation in artificial brine/recovered solution, the purity of the recovered solution reached 94.59 % (Fig. 7b).

Additionally, Zhou et al. [63] firstly used carbon-coated $Li_3V_2(PO_4)_3$ (LVP@C) as the cathode electrode (Fig. 7c). The optimized Li^+ extraction capacity of LVP@C reached a maximum of 25.8 $mg{\cdot}g^{-1}$ and maintained a high retention rate of 78 % after 50 cycles. The Li^+ selectivity coefficients at high Mg-Li and Na-Li ratios of 1:5 and 1:15 were 444.7 and 351.2, respectively. Electrode materials directly impact Li^+ extraction performance, including capacity, reversibility, and stability. Improving material conductivity, increasing surface area, and optimizing structure can enhance Li^+ adsorption and release rates. Various materials, such as LMO and LFP, have been studied and developed for Li^+ extraction from salt lake brines [64,65]. To improve storage capacity, cycling stability, and ion selectivity, the following strategies have been applied: (1) Material modification, which includes doping, coating, surface treatment, and pore engineering, as well as the structural optimization of the crystal structure, microstructure, macrostructure, and chemical composition of existing active materials; and (2) the bespoke development of new active materials for working electrodes, tailored to the complex compositions of distinct brine systems [28,66].

2.2. Study on the optimum design and kinetic performance of reaction tank

2.2.1. Optimal design of reaction tank

The reaction tank of traditional electrochemical systems consists of enrichment liquid and brine chambers, selectively capturing and enriching Li^+ from salt lake brines. Most traditional ELE systems adsorb Li^+ from the anode, then wash the electrode, and finally energize the electrode to release Li^+ into the enrichment solution [67]. This process is inefficient, consumes large amounts of fresh water, and faces issues with electrode amplification, exchange difficulties, and impurity ion attachment [68,69]. To solve these problems, researchers have made

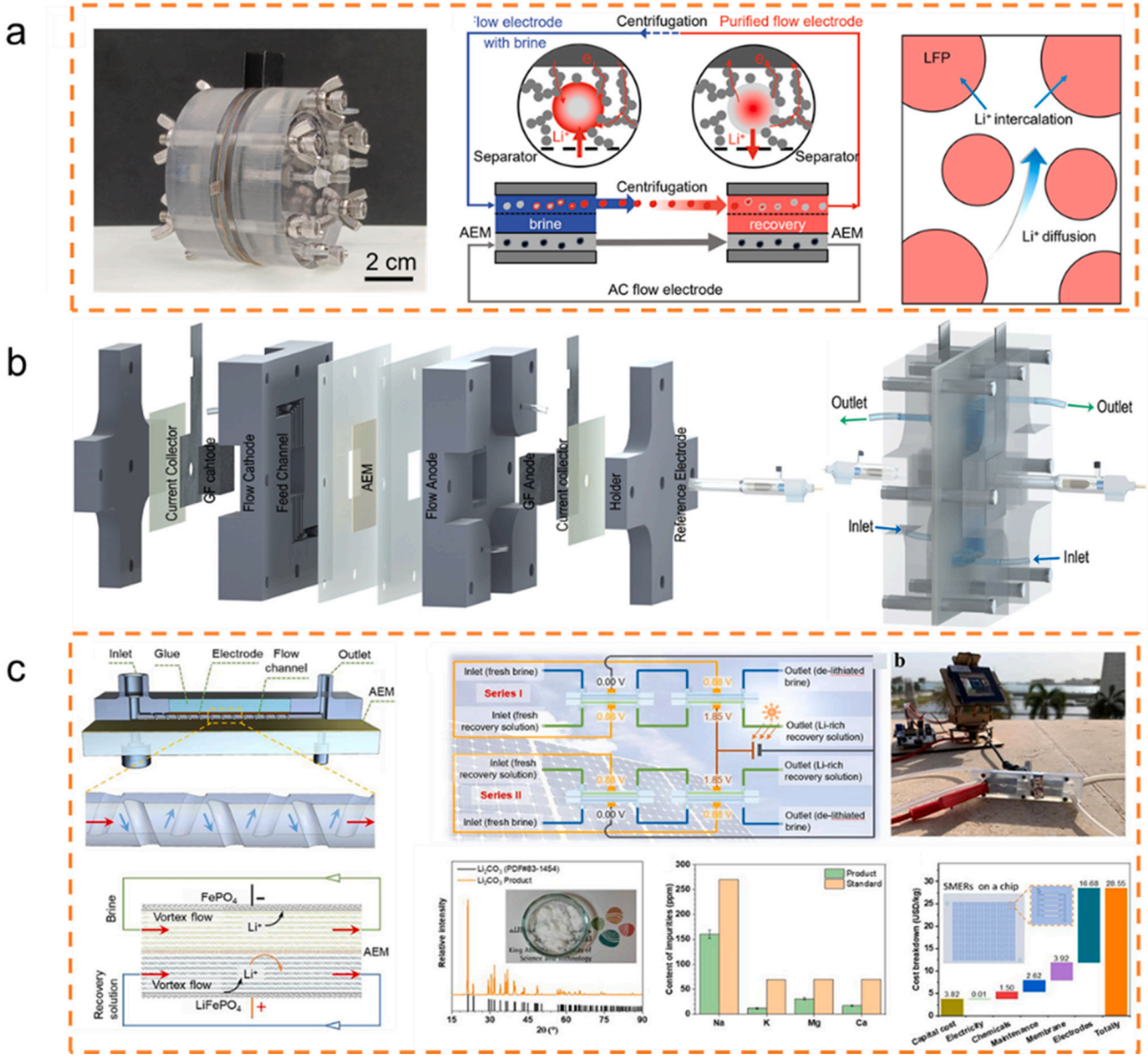

Fig. 8. Reaction tank structure diagram. (a) Schematic diagram of ELE system of flow electrode and mechanism of enhancing mass transfer of flow electrode. Reprinted with permission [70], copyright 2024, Elsevier. (b) Schematic diagram of flow type Li^+ recovery device. Reprinted with permission [47], copyright 2021, Elsevier. (c) Schematic of the scalable spiral microstructured electrochemical reactor and schematic of the solar-powered upgrade system. Reprinted with permission [71], copyright 2023, Elsevier.

significant contributions to system optimization.

Traditional solid electrodes have limited capacity due to their low loading of active materials. For example, Zhu et al. [70] designed an ELE system with continuous flow electrodes. This flow system includes Li^+ adsorption, purification of the LFP flow electrode, and Li^+ desorption (Fig. 8a). The suspension of active particles significantly enhances the density of the active particle/electrolyte interface and decreases the migration distance for Li^+. In a flow electrode system, all active materials flowing through the electrode contribute to Li^+ adsorption and desorption, leading to a lower current density per unit of active material compared to solid electrodes. This reduced current density lessens polarization during Li^+ intercalation at the particle surface, thereby improving kinetic properties. Additionally, Wang et al. [47] designed a flow-type Li^+ recovery device (Fig. 8b) to effectively reduces the concentration polarization of brine, increase reaction area, shorten the mass transfer distance of the liquid phase, and use constant pressure to save energy, allowing for stable Li^+ de-intercalation. Zhang et al. [71] designed a scalable helical microstructure ELE reactor (SMER, Fig. 8c) to achieve ultra-fast and economical Li^+ extraction through significantly accelerated mass transfer under complex brine conditions. The solar drive is used to achieve economic, ultra-fast Li^+ extraction with SMER. SMER's Li^+ extraction rate is 5.6 times higher (21.96 $mg{\cdot}g^{-1}{\cdot}h^{-1}$) while maintaining high product purity.

In general, studying the structure of the flow electrode is of greater concern than studying the fluidity of the electrode material. A more compact tank structure minimizes the distance between the electrodes, reducing the ohmic drop and system volume [72]. In flow electrode design, brine is pumped via the porous matrix of the electrode, increasing convective flow along the thickness of the electrode stack and improving mass transfer in the pores. For example, Romero et al. [73] designed an electrochemical reaction tank for sustainable lithium extraction consisting of two 3D porous filled bed electrodes and a porous diaphragm filled with electrolytes. The electrodes are filled with conductive petroleum coke particles and covered with LMO polypyrrole, which is selective to lithium ions and anions, respectively. It operates in two steps: First, porous electrodes and partitions are filled with natural brine to extract Li^+ and Cl^- by intercalation and adsorption. Then, after rinsing with water, the reactor is filled with dilute LiCl recovery solution and LiCl is recovered by reversing the current. Additionally, the liquid resistance of the down-flow structure is lower than that of the straight-through structure (Fig. 9a). This reactor is suitable for low Li^+ concentration brines (0.5–70 $mg{\cdot}L^{-1}$), as the circulation of the brine in the reactor enhances Li^+ transport from liquid to solid.

Kim et al. [74] reported a hybrid supercapacitor system for Li^+ recovery in a flow electrode reactor, using λ-MnO_2 as the Li^+ capture electrode and activated carbon to capture Cl^-. The electrodes are placed inside a cylindrical reactor (Fig. 9b), forming a sandwich structure through which air flows. The system captures Li^+ from synthetic Atacama brine at a concentration of about 90 mM. Demonstrated a fairly low level of energy consumption (4.2 Wh $mol{\cdot}Li^{-1}$). Additionally, the excellent stability of the hybrid supercapacitor lithium recovery system was demonstrated through continuous operation of up to 50 cycles. Meanwhile, Wang et al. [75] designed a flow ELE system with a porous gas flushing operation, demonstrating that multiple gas cleaning operations can significantly reduce ultra-pure water consumption during solution exchange (Fig. 9c) because ELE systems require a continuous

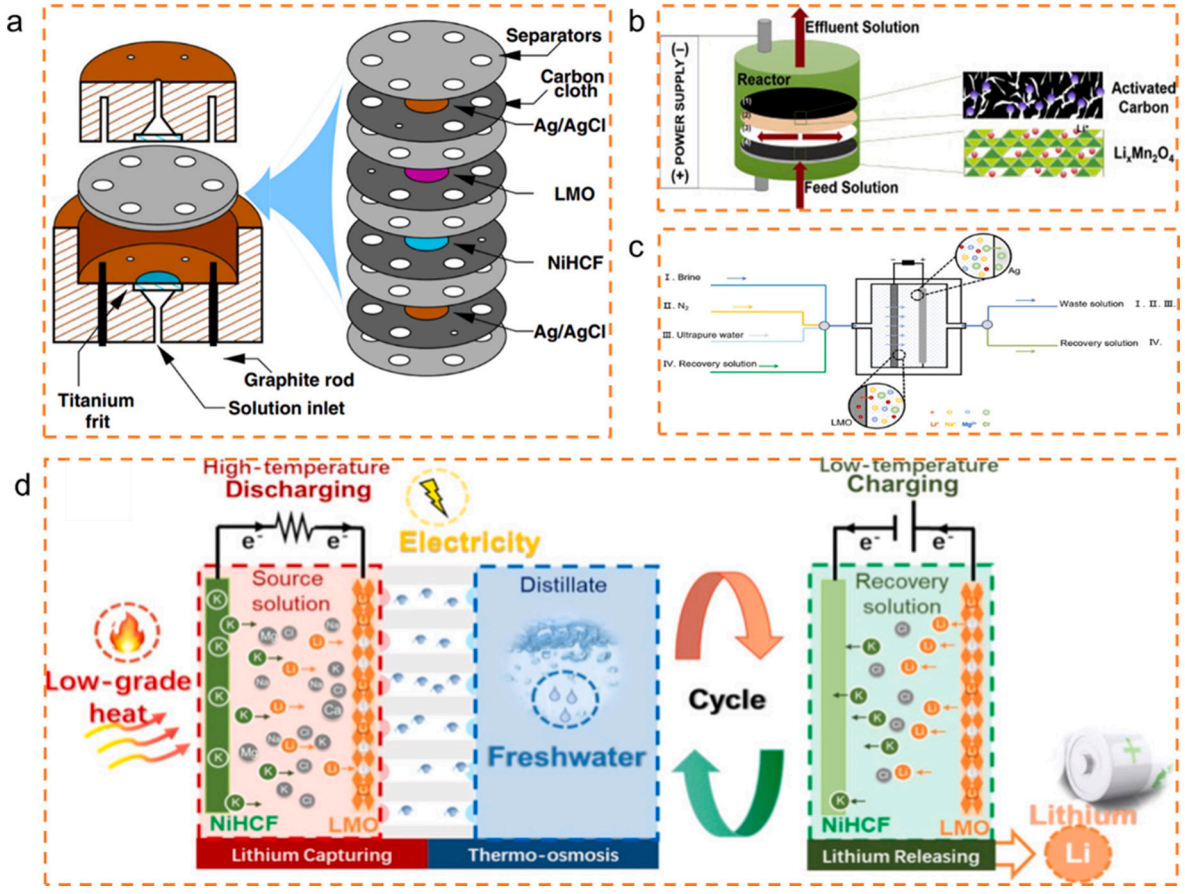

Fig. 9. Schematic diagram of porous flow electrode (a) Schematic digram of the porous flow electrode system. Reprinted with permission [72], copyright 2017, Elsevier. (b) Schematic diagram of Li^+ extraction from a flow electrode system with sandwich structure. Reprinted with permission [74], copyright 2015, Elsevier. (c) Schematic diagram of porous gas flushing ELE system. Reprinted with permission [75], copyright 2023, MDPI. (d) Schematic illustration of the coupled system. Reprinted with permission [76], copyright 2021, PubMed.

output of Li^+ sources and energy.Among them, the average energy consumption of Atacama simulated salt Lake water as the source solution is 0.732 $kWhkg^{-1}$ Yuan et al. [76] demonstrated a fast, energy-efficient, and environmentally friendly lithium production system that combines thermal regenerative electrochemical cycling (TREC) with polyvinylidene fluoride film thermal permeation (TO-TREC) using LMO and nickel HHCF electrodes (Fig. 9d). The yield rate of Li^+ was 50–60 $mmol{\cdot}m^{-2}{\cdot}h^{-1}$. TREC collects thermal energy from heated saltwater, saving over 20 % of electrical energy compared to traditional electrochemical methods. This system shows the potential to meet the growing global demand for lithium in many applications. This research on optimizing reaction tanks presents various design concepts aimed at enhancing the efficiency of Li^+ extraction in ELE systems, as well as promoting environmental sustainability and economic benefits. Nonetheless, the design of a reaction chamber encounters practical challenges related to industrialization, including complex scaling effects and issues of feasibility [66]. Therefore, future research can focus on reactor engineering, system expansion, and technical economics to design a reaction tank with these advantages.

2.2.2. Study on kinetic properties

In ELE, several process parameters affect the system's kinetic performance, including cell voltage, reaction temperature, and electrode construction [77]. The cell voltage plays a crucial role in determining the rate of chemical reactions, which directly influences the efficiency and cost of Li^+ extraction. At low cell voltages, the reaction rate is slow, allowing Li^+ ions in the solution to sufficiently replenish the lithium consumed within the electrode, with the process primarily governed by chemical reaction kinetics. In contrast, as the voltage increases, the reaction rate accelerates, leading to rapid consumption of Li^+ at the interface of unreacted particles. This swift consumption inhibits the timely replenishment of lithium from the bulk solution, resulting in a reaction that becomes limited by internal diffusion. For example, Zhao et al. [78] used the contraction kernel model for kinetic fitting analysis and found that as cell voltage increases, the control steps of the lithium extraction reaction gradually shift from chemical reaction control to internal diffusion control. To ensure minimal competition from impurity cations, a moderate increase in tank voltage can speed up the reaction. However, improper potential control can lead to problems such as impurity ion intercalation and brine decomposition. Therefore, optimizing the potential, reducing energy consumption, and improving current efficiency are key issues for enhancing Li^+ extraction efficiency. Relative research progress in this area is list below.

Hong et al. [79] used cyclic voltammetry (CV) to test the electrochemical performance of NCM materials during Li^+ extraction and found that reducing the current mode can decrease the concentration polarization of Li^+ on the electrode surface, thereby improving lithium de-incarceration efficiency. They determined optimal values for current density and frequency at 0.5 $mA{\cdot}cm^{-2}$ and 0.5 Hz, respectively (Fig. 10a). In addition, Guo et al. [30] examined the performance of an electrochemical de-lithiation system using $LiMn_2O_4/Li_{1-x}Mn_2O_4$ under constant current and constant voltage modes. The researchers observed that in constant current mode, the potential increased over time, which resulted in reduced energy consumption and lower Li^+ extraction capacity. Conversely, in constant voltage mode, the potential remained stable, resulting in higher energy consumption but enhanced lithium extraction capacity. To optimize this process, they developed a method that initiates Li^+ extraction in constant current mode until the potential reaches a predetermined threshold, after which the system switches to a constant current-constant voltage (CC-CV) mode. This approach aims to improve Li^+ extraction efficiency while minimizing changes in electrode polarity (Fig. 10b). Additionally, Liu et al. [80] used a pulse pause method (10 s pause, 10 s intercalation) for Li^+ extraction, which showed superior results compared to the constant current method. They

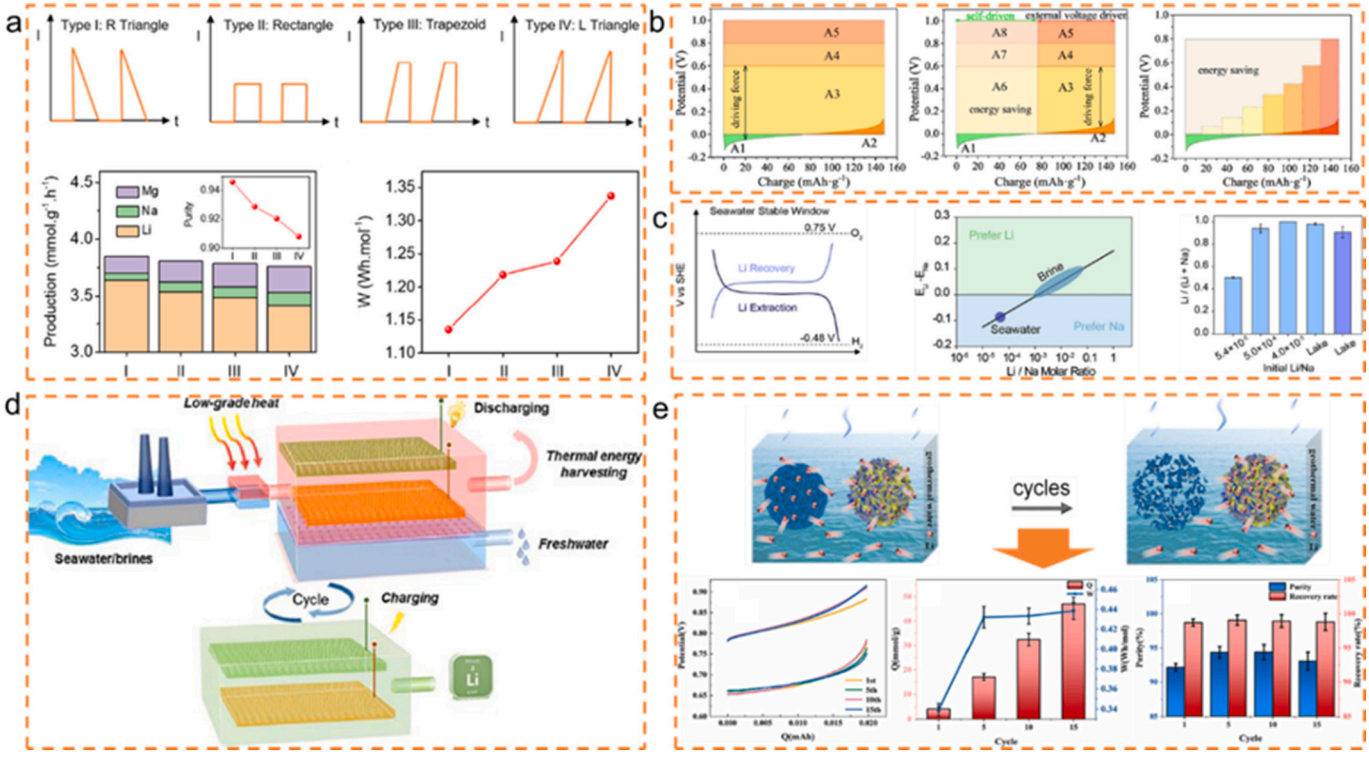

Fig. 10. Potential and temperature optimization measures. (a) The results of ELE under different discharge curves. Reprinted with permission [79], copyright 2022, Elsevier. (b) Analysis of energy consumption of Li^+ extraction under different driving modes. Reprinted with permission [30], copyright 2022, Elsevier. (c) Using pulse pause method to improve Li^+ extraction performance. Reprinted with permission [80], copyright 2020, Elsevier. (d) Schematic diagram of thermal assisted Li^+ extraction process. Reprinted with permission [81], copyright 2022, Elsevier. (e) Li^+ extraction performance of $LiMn_2O_4$-Pyr-2D composite electrode in Tibetan geothermal water at 60 °C. Reprinted with permission [86], copyright 2023, Elsevier.

concluded that the pulse pause method provides rest periods for the electrode, allowing Li^+ and Na^+ to redistribute among all particles in the electrode. This leads to a more uniform lithium-sodium content across particles, improving electrode uniformity and reducing intercalation overpotential (Fig. 10c).

The change of temperature also has a significant impact on the electrochemical removal efficiency of Li^+. Zhao et al. [78] found that increasing the temperature markedly improved both the adsorption capacity and rate of lithium by the electrode material. For instance, the adsorption capacity over 5.5 h was only 25 $mg{\cdot}g^{-1}$ at 10 °C, whereas the adsorption capacity reached 32 $mg{\cdot}g^{-1}$ at 50 °C within 3 h. Similarly, Yu et al. [81] discovered that Li^+ extraction was influenced by both temperature and concentration. In a heated source solution, the Li^+ extraction capacity (i.e., the mass of Li^+ extracted from the source solution) and the velocity (i.e., the extraction rate of Li^+) were significantly increased (Fig. 10d). Higher temperatures (e.g., 60 °C) reduced the activation polarization of Li^+ intercalation, decreased the charge transfer resistance, and promoted the diffusion of Li^+. According to the Stokes-Einstein equation, temperature is positively correlated with the diffusion coefficient of ions [82,83]. However, the temperature resistance of the material is also a crucial factor. For example, LMO exhibits considerable capacity degradation under high-temperature conditions. The failure mechanisms at elevated temperatures include: (1) the Jahn-Teller effect, and (2) the dissolution of Mn, where Mn^{3+} ions on the particle surface are readily polarized during charging and discharging, resulting in the dissolution of Mn^{2+} ions into the brine and leading to irreversible capacity loss. Consequently, regulating the temperature appropriately can enhance Li^+ extraction efficiency while reducing the risk of material degradation. When Li^+ is extracted from high-temperature geothermal water, extensive treatment is required to regulate the water to the proper temperature, resulting in longer processing times, increased energy consumption, and higher costs [84,85]. To address these challenges, researchers have implemented various strategies. For instance, Zhao et al. [86] designed a $LiMn_2O_4$-Pyr-2D composite electrode material. This material has the characteristics of orderly and stable molecular structure, regular pores, and evenly distributed elements. Such a design effectively slows down the dissolution rate of Mn at high temperatures and mitigates the collapse of the LMO structure caused by the Jahn-Teller effect. Consequently, this significantly enhances the high-temperature resistance of LMO. After leaching Li^+ 20 times in geothermal water at 60 °C, the capacity retention rate was 92.52 %, and the unit energy consumption was 0.46 $Wh{\cdot}mol^{-1}$ (Fig. 10e).

Finally, the construction of electrodes is also an important factor affecting the kinetics of Li^+ extraction from brine, which involves complex electrochemical reaction processes and engineering challenges [87]. In the ELE process, High-load electrodes are critical for the industrialization of lithium extraction; however, several challenges impede their effectiveness. The high viscosity and calcification of salt lake brine hinder its penetration through increased electrode thickness, leading to a reduction in Li^+ extraction efficiency near the current collector. Additionally, significant active material loading can cause localized Li^+ accumulation, resulting in concentration gradients that induce concentration polarization. Furthermore, as the content of electrode materials increases, the uneven distribution of conductive additives and brine within thickened electrodes disrupts ion and electron transfer, causing electrochemical polarization and further diminishing Li^+ extraction efficiency [88]. To address these issues, our research group developed high-load electrodes (20 $mg{\cdot}cm^{-2}$) using 3D-reduced graphene oxide (rGO) and metal foam (MF) to construct a three-dimensional conductive network in situ, significantly enhancing Li^+ dynamics and solving high-load electrode efficiency issues in salt lakes for the first time (Fig. 11a) [67,88,89]. Furthermore, Zhao et al. [68] prepared a high-performance porous electrode using polyethylene glycol (PEG) as a template (Fig. 11b), achieving a coulomb efficiency of 98.5 % over 1000 cycles at a high current density of 30 $A{\cdot}m^{-2}$ with a stable cycle performance.

At present, ELE's research is mainly focused on material selection, concentration, and purity of recovery liquid and reaction efficiency to improve Li^+ selectivity [35,90]. There are relatively few researches on the improvement of the reaction tank. The design of the reaction tank is also important for improving the efficiency of Li^+ extraction and reducing energy consumption. Optimizing the design of the reaction tank, such as enhancing the contact area between the electrode and the brine and minimizing the distance between the electrodes, can effectively reduce internal resistance in the electrolytic process, resulting in improved current density and energy efficiency [72]. In addition, the development of new reaction tank designs, such as flow batteries and microfluidic reaction tanks, is also an effective way to improve ELE performance. Process parameters of the reaction tank critically influence Li^+ extraction performance [26]. For instance, the electrolytic temperature boosts the migration rate of Li^+, but overly high temperatures may decompose the electrolyte and degrade the electrode material. Thus, it is necessary to consider the material's temperature tolerance carefully. Additionally, the choice of potential, linked to the material structure, varies by material. Optimizing the duration of potential application can conserve energy and enhance current efficiency while maintaining Li^+ adsorption capacity. Moreover, the interplay between Li^+ adsorption capacity and Li^+ transport kinetics, facilitated by proper electrode construction, is crucial for improving Li^+ extraction efficiency. Overall, Improving the performance of ELE necessitates a holistic approach that integrates materials science, chemical engineering, and electrochemistry. By optimizing the brine or concentrated solutions, electrode materials, reactor design, and operating conditions, lithium extraction efficiency can be markedly enhanced, production costs can be reduced, and the sustainable development of electric vehicles and mobile devices can be advanced. Additionally, the continuous development of novel materials and technologies offers significant research opportunities and promising future applications in the ELE field.

2.3. Study on pretreatment of brine in salt lake

In the ELE system, operating at low voltage and high current is widely acknowledged as the most ideal approach for Li^+ extraction due to its low energy consumption and high current efficiency. However, due to polarization voltage, the actual operating voltage must exceed the embedded Li^+ potential. Polarization is particularly pronounced in low-grade brines, which contain fewer Li^+ ions and more impurity ions, leading to severe concentration polarization. Furthermore, the high concentration of SO_4^{2-} in the mother liquor of certain brines increases the transmembrane resistance, potentially pushing the operating voltage beyond the brine's original decomposition voltage (as illustrated in Eq. (6)). When polarization is severe, it is easier to exceed this threshold and there is a risk of chlorine gas being produced in the chlorinated brine and changing the system pH, thereby corroding the electrodes. It requires effective brine pretreatment to resolve these issues. Given that the principles of ELE systems are very similar to water-based lithium-ion batteries, the electrolyte treatment and electrochemical impurity embedding strategies found in water-based batteries can be applied. Implementing these strategies can optimize brine formulations and provide multiple options for future modified brine electrolytes.

$$E = E_1 + E_2 \tag{6}$$

E is the voltage applied by the system; E_1 is open circuit voltage/polarization voltage; E_2 is the actual lithium drive voltage [91].

Due to the existence of polarization voltage, the application of high-concentration phase brine is greatly limited. Therefore, we learned from the water-based Li-ion battery electrolyte-related high voltage strategy to improve the decomposition voltage of brine: (1) Additive strategy: select substances that can catalyze or participate in SEI generation as additives, such as trimethylsilyl borate (TMSB), acrylamide (AM), urea, CO, etc. [92,93]; (2) Co-solvent strategy: Organic solvents with low

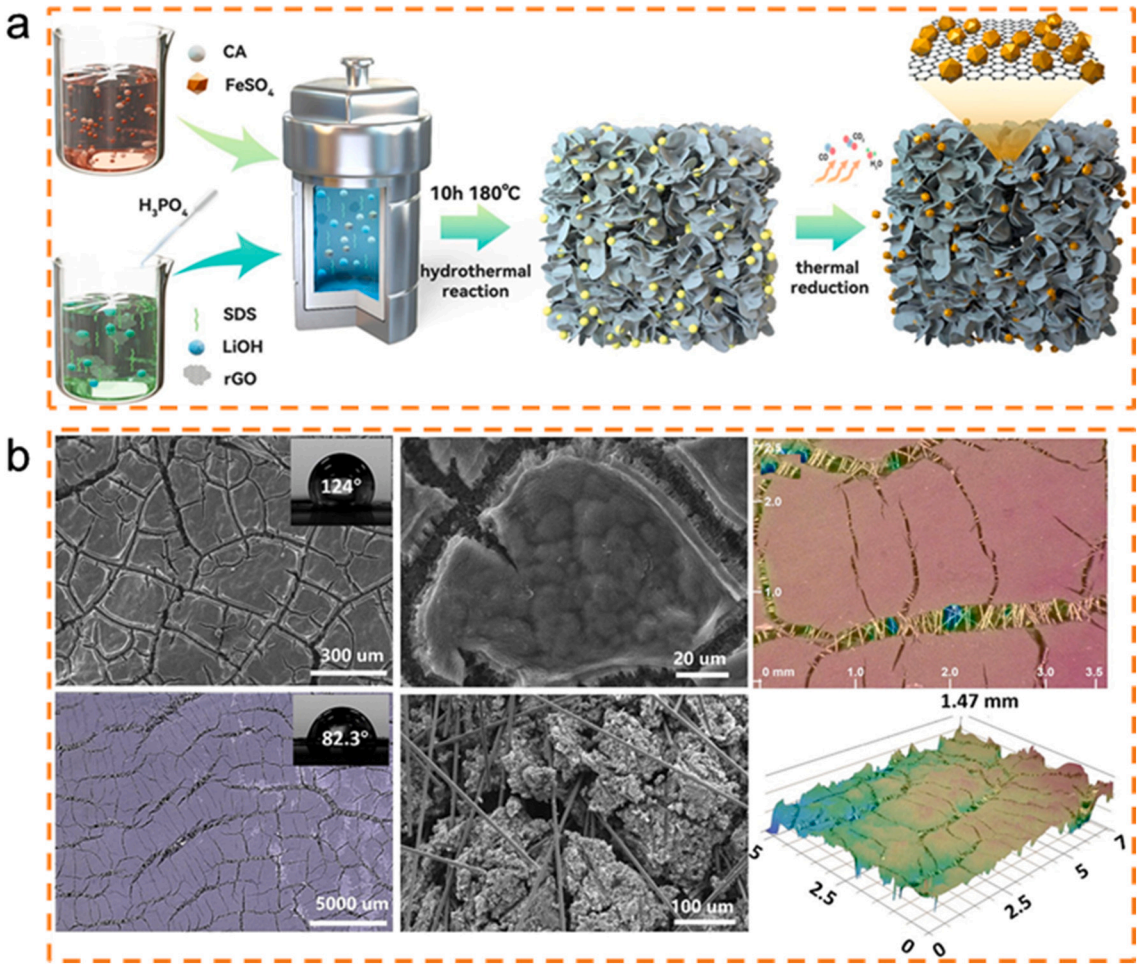

Fig. 11. Electrode construction. (a) Schematic diagram of LFP/rGO electrode preparation. Reprinted with permission [88], copyright 2024, Elsevier. (b) Surface morphology of PVDF-$LiFePO_4$ and PEG modified porous $LiFePO_4$ electrode materials. Reprinted with permission [68], copyright 2023, Elsevier.

viscosity, high dielectric constant and low inflammability are selected as co-solvents to regulate the solvation structure of ions, and local high-concentration electrolytic solution is constructed, such as dimethyl carbonate (DMC), acetonitrile (AN), dimethyl sulfoxide (DMSO), polyethylene glycol (PEG), sulfoxide (SL), etc. [94,95] The aforementioned strategy will enhance the electrochemical window from both thermodynamic and kinetic perspectives. The introduction of additional additives or co-solvents yields the following effects: (1) Water molecules predominantly form strong coordination with cations, establishing hydrogen bonds with the additives or co-solvents. This modification of the chemical environment results in an increased HOMO-LUMO gap of water molecules and a decrease in water activity. Additionally, the hydrogen bonds formed between certain additives and water molecules are weaker than those between the water molecules themselves, which strengthens the O-H bonds in the water molecules and improves thermodynamic stability [92,93]. (2) Anion/additive/co-solvent molecules also participate in cationic solvation, and the intermolecular interaction is enhanced. The change of chemical environment leads to the REDOX reaction of anion/additive/cosolvent molecules will be superior to HER/OER. The solid product obtained from the reaction forms the electrode-electrolyte interface layer, which hinders the direct contact between the electrode and the electrolyte, increases HER/OER overpotential, and inhibits the decomposition of the brine [94,95].

2.4. Brine impurity removal strategy

Salt lake brine is a complex aqueous phase containing major cations such as Li^+, Na^+, Mg^{2+}, K^+, and Ca^{2+}. Experimental investigations have revealed that impurity ions become more prominent at higher concentrations and can be selectively removed by the lattice of the electrode material. After the selective insertion of Li^+, these impurities accumulate on the electrode surface, resulting in the simultaneous consumption of Li^+ and replenishment of impurity ions on the same side of the electrode. This process affects the reaction rate by increasing in-situ resistance and internal voltage, leading to concentration polarization. Furthermore, when voltage is applied, a double electric layer forms at the negative electrode. As Li^+ ions are inserted into the electrode, ions from the boundary layer replenish this layer, creating a new double electric layer with low Li^+ concentration and high impurity ion concentration. This accumulation of impurity ions in the boundary layer enhances their likelihood of reaching the electrode surface, thereby obstructing the migration of Li^+ [91]. Thus, effectively removing brine impurities is crucial. This summary outlines de-hybridization strategies for ELE systems that focus on enhancing the relative content of Li^+ to improve Li^+ extraction efficiency.

We believe that electrolysis can mitigate the impact of certain impurities from the outset of production. For instance, Lalia et al. [96] showcased a two-step electrochemical process for the selective separation and recovery of calcium and magnesium from brine (Fig. 12a). The initial step involves carbon dioxide removal from the brine while electrochemically precipitating calcite at a titanium dioxide-coated graphite cathode and the original graphite anode at 2.5 V. The titanium dioxide coating effectively enhances selective calcite precipitation. Following this, brucite is selectively precipitated at the same electrodes at 3.5 V,

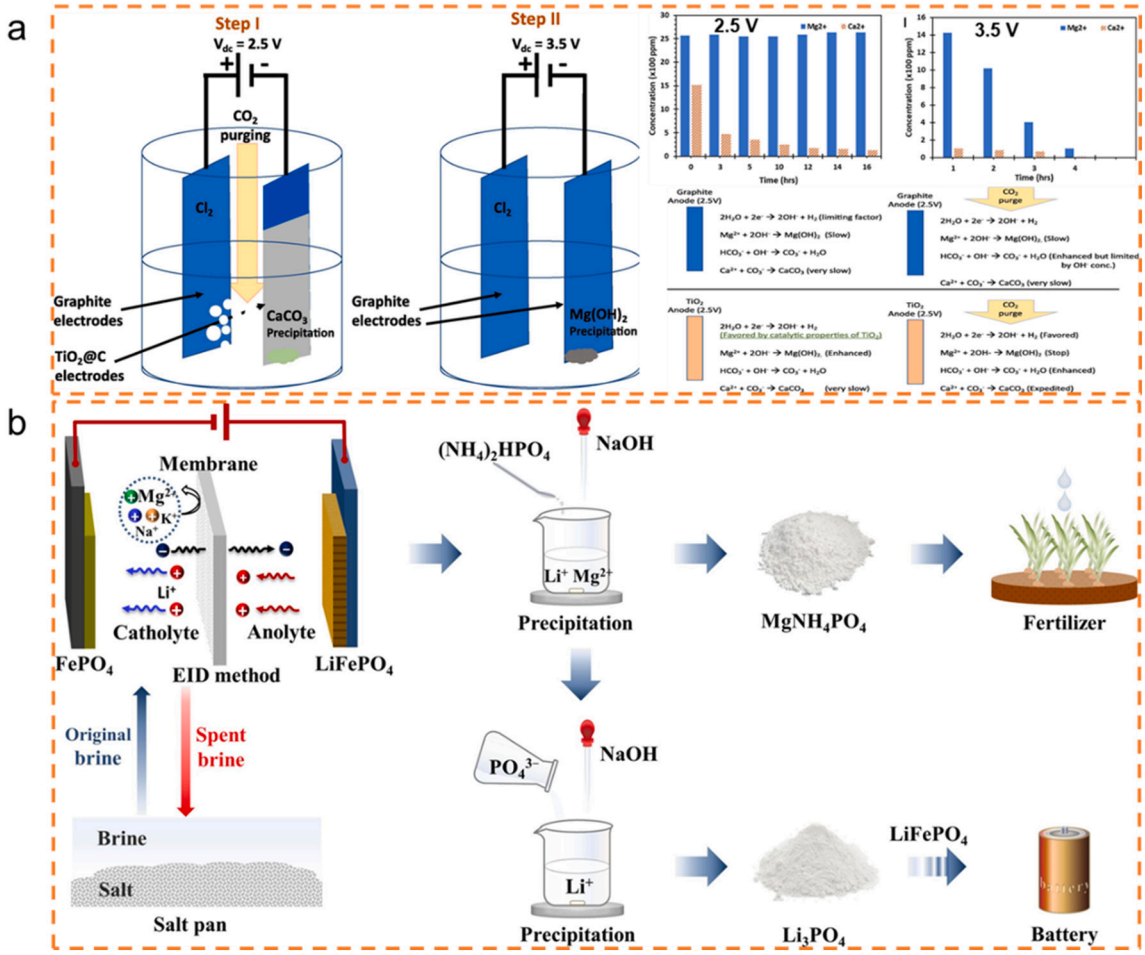

Fig. 12. Related strategies of brine impurity removal. (a) Schematic diagram of electrochemical cell device, mechanism diagram and electrolysis results for selective precipitation of calcite (Step I) and brucite (Step II). Reprinted with permission [96], copyright 2021, Elsevier. (b) By means of EID-$MgNH_4PO_4$ coupling precipitation technology, Li^+ was directly extracted from brine and the flow diagram of Li_3PO_4 was obtained. Reprinted with permission [97], copyright 2023, Elsevier.

facilitating the precipitation of Ca^{2+} and Mg^{2+} and reducing competition from impurity ions. Integrating this method with ELE could significantly reduce impurity ion interference and increase the purity of the recovered Li^+ liquid. Additionally, Ju et al. [97] introduced a method coupling electrochemical de-scalation with ammonium magnesium phosphate precipitation (Fig. 12b) to directly extract Li^+ from brine and produce Li_3PO_4. After removing Mg^{2+}, the concentration of Mg^{2+} in the anodic solution is reduced to 3 ppm, with a Li^+ loss rate of $<$1.9 %. This suggests potential cross-application of these research findings in the future, aiming to diversify this field of study.

2.5. *Electrochemical coupling with other technologies to improve the efficiency of lithium extraction*

Electrochemical technology offers a cost-effective, flexible, environmentally friendly, and convenient operation for recovering Li^+ from liquid ore, presenting broad application prospects [98]. However, due to the limitations of single electrochemical methods, there is increasing interest in combining various electrochemical techniques or combining them with other types of techniques to create synergistic effects. This multi-technology combination opens up new opportunities for the extraction of Li^+.

Currently, most studies focus on reducing energy consumption to address the limitations of electrochemical lithium extraction methods. For instance, Cui et al. [99] proposed an efficient electrochemically coupled electrolysis method for the continuous extraction of lithium from salt lake brine. This approach leverages zero equilibrium voltage and low overpotential during hydrogen precipitation and oxidation reactions, achieving a high Faraday efficiency of 88.87 % and lithium selectivity of 0.9954 at an operating voltage of only 0.25 V. Compared to traditional lithium mining methods, this RCE technology significantly lowers energy consumption and costs while minimizing environmental impact. Additionally, Yuan et al. [76] designed a system that integrates thermal osmosis and thermal regeneration electrochemical cycling for efficient and rapid lithium extraction. By utilizing a low-quality heat source, the thermal osmosis system concentrates low-concentration lithium-containing raw water (e.g., reverse osmosis concentrate from seawater desalination and industrial wastewater) at a much higher rate than traditional solar evaporation. Concurrently, it generates high-purity water as a byproduct. The electrochemical system then extracts and recovers lithium from the heated and concentrated raw water with high selectivity. The thermal regeneration electrochemical cycle involves transferring the electrode from the high-temperature lithium-containing water to a standard temperature recovery solution, releasing lithium and enabling the recovery of high-purity lithium chloride. This process also converts thermal energy into electrical energy, further reducing the electrical energy consumption of the electrochemical process.

Recent advances in the use of electrochemical methods and traditional technologies for Li^+ extraction include a noteworthy proposal [100]. Additionally, electrochemical coupling with traditional methods has also made good progress. They introduced an ion “distillation” technique using multiple membrane stacks (Fig. 13a), significantly enhancing the selectivity of Li^+ by several orders of magnitude. The

process begins with an initial pretreatment to remove coexisting ions from the brine, followed by obtaining an enriched Mg^{2+}/Li^{+} solution which is then subjected to ion distillation. This method achieved selectivity ratios of 26,177 for Mg^{2+}/Li^{+} and 27,000 for Cl^{-}/SO_4^{2-}. Zhao et al. [101] developed an integrated membrane series process that combines bipolar membrane electrodialysis (BMED) with nanofiltration (NF), reverse osmosis (RO), and precipitation (ED) to produce LiOH from salt lake brine. This method is especially effective for separating, concentrating, and extracting Li^{+} from brines with high Mg^{2+}/Li^{+} ratios (Fig. 13b). Initially, the filter membrane removes significant amounts of Ca^{2+} and Mg^{2+} from the brine. The resultant osmotic solution is then enriched through an integrated RO-ED process. LiOH is prepared after treating the BMED feed solution with a precipitation method, followed by evaporation crystallization. This process reduces the Mg^{2+}/Li^{+} ratio from >30 to 0.5, increases Li^{+} concentration to 14 $g{\cdot}L^{-1}$, and achieves a Li^{+} recovery rate exceeding 92.0 %. The concentrated LiOH solution reaches over 1.0 $mol{\cdot}L^{-1}$, with a current efficiency of 36.05 % and energy consumption of 6.20 $kWh{\cdot}kg^{-1}$.

Han et al. [102] introduced a coupling technique combining membrane distillation (DCMD) with Electrically Switchable Ion Exchange (ESIX) (Fig. 13c) to enhance the simultaneous enrichment of SWRO brine and selective Li^{+} recovery. This approach increased the freshwater recovery rate from simulated SWRO seawater by 12 % and boosted the Li^{+} concentration by 2.4 times. The effectiveness of mixed-mode operation in Li^{+} enrichment from simulated saline solutions is highlighted. Meanwhile, Zhao et al. [103] first utilized the high selectivity of Electrodialysis Ion Exchange (EDI) to extract lithium from saltwater, subsequently preparing LiCO through precipitation. The sodium content of the resulting LiCO is only 154 × 10 wt%, meeting the standards for battery-grade lithium carbonate. The lithium recovery rate for each process exceeds 87 %, with an overall recovery rate of 74.93 %.

Some limitations of electrochemical lithium extraction can be addressed by coupling two or more technologies. While the feasibility of extracting lithium from brine has been demonstrated at the laboratory stage, the coupling of these technologies remains in the research phase. It is essential to focus on the economy, effectiveness, and stability of the lithium extraction process from salt lake brine to facilitate the expansion of production scale. Establishing a pilot-scale production line will ensure that the equipment operates effectively over time, aiding in its gradual industrialization. Additionally, attention must be given to the research and development of new technologies to overcome key bottlenecks. This includes developing comprehensive methods for treating high-salinity wastewater and improving lithium resource extraction technologies. Furthermore, advancing lake halogen lithium extraction technologies should prioritize efficiency, simplicity, and environmental protection.

3. Challenges

The Li^{+} extraction properties of materials are involved in various electrochemical methods (Table 2). Although ELE has made great progress over the past decade, some challenges remain. In this section, we will cover the most pressing issues regarding ELE systems, including analysis of the causes of inefficiency, the challenge of competing impurity ions, and energy costs.

3.1. Low efficiency analysis

3.1.1. Material intrinsic properties

During ELE, active materials need to have both good ionic and electronic conductivity to ensure efficient lithium-ion transport and rapid electron transfer [117]. However, the performance of many active materials in these two aspects is relatively insufficient, directly affecting

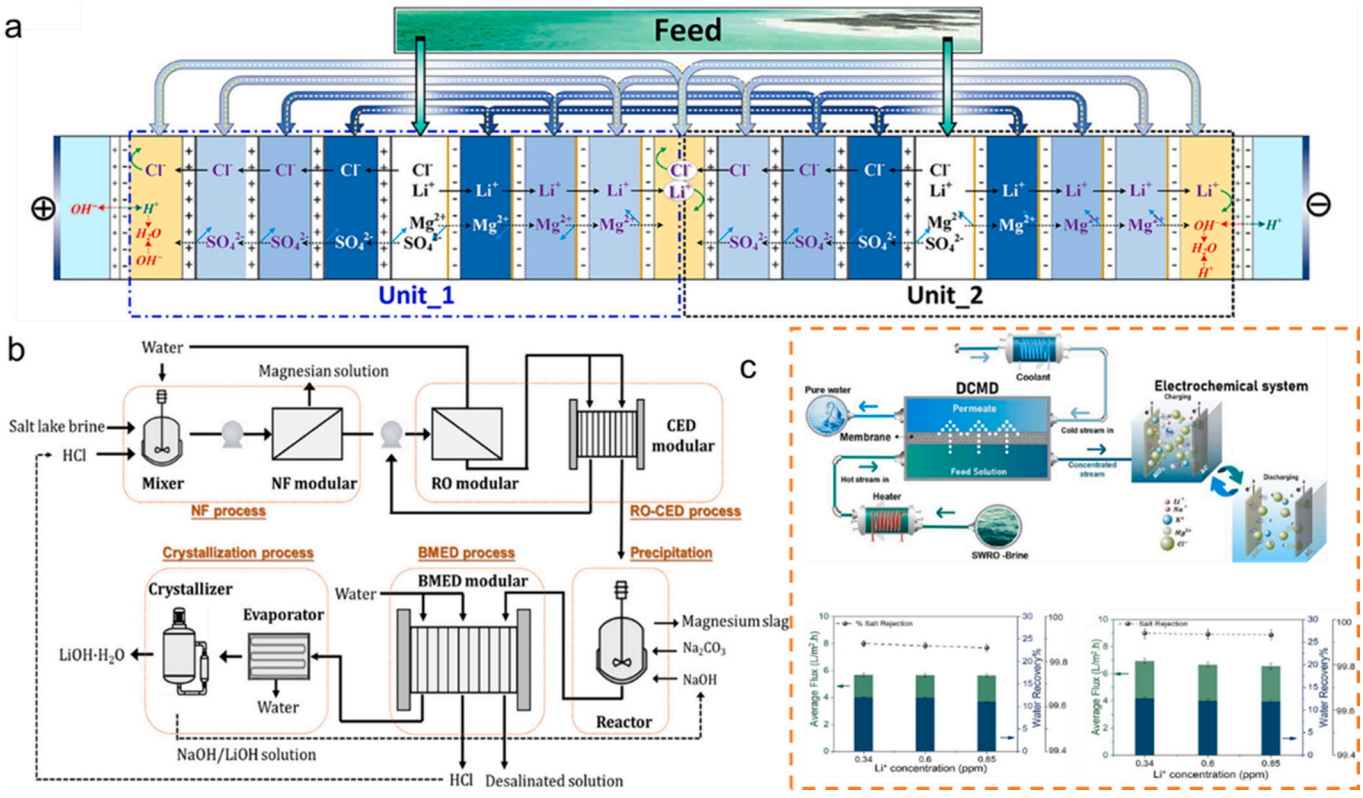

Fig. 13. Multi-technology coupling measures. (a) Changes in ion composition and lithium selectivity during four-stage ion "distillation" treatment of lake brine. Reprinted with permission [100], copyright 2022, Wiley. (b) Principle of integrated membrane method [101]. Copyright 2020, Elsevier. (c) Schematic diagram of an experimental method for the DCMF-ESIX hybrid system used to recover Li^{+} from artificial reverse osmosis brine. Reprinted with permission [102], copyright 2024, Elsevier.

Table 2
Comparison of Li^+ extraction performance of each electrode system.

Electrode materials	M/Li^+	$M1/Li^+$	Performace	Capacity retention rate ($mg \cdot g^{-1}$) - after cycles	EC($Wh \cdot mol^{-1}$)	Ref
LFP	Mg/Li = 484	Mg/Li = 0.5	25	84 % - 50 cycles		[104]
LMO	Mg/Li = 58.8	Mg/Li = 1.7	15.7	91 % - 100 cycles	16	[11]
porous LMO	Mg/Li = 61	Mg/Li = 1.08	20	87.04 % - 120 cycles	8.74	[105]
crack-porous LFP	Mg/Li = 62.2	Mg/Li = 0.5	30	90 % - 100 cycles		[68]
$LFP/L_{0.3}FP$	Na/Li = 138	Na/Li = 1.33	25	90 % - 100 cycles		[106]
LFP/Olivine-FP	Mg/Li = 54.2	Mg/Li = 1.65	32	87.5 % - 120 cycles		[107]
rGO-LFP	Mg/Li = 65.6	Mg/Li=	32.12			[89]
MF-LFP	Mg/Li = 65.6	Mg/Li = 0.47	25.34			[88]
LFP	Mg/Li = 3.2	Mg/Li = 0.04	94.81 %*			[103]
	Na/Li = 37.7	Na/Li = 2.45				
LiNi0.025Co0.025 Mn1.95O4	Mg/Li = 38.46	Mg/Li = 1.05	99 %*		3.97	[62]
Tr-oh LMO	Mg/Li = 1	Mg/Li = 0	20.25	85.2 % - 30 cycles	1	[108]
Ag /λ-MnO_2 /PPy/PSS	Na/Li = 1	Na/Li = 0.22	30		1	[109]
LMO			24.29			[87]
rGO-H1.6Mn1.6O4			38.781			[17]
LMO	Na/Li = 20,000		λ/7644	–	10–30	[110]
LNCMO	Mg/Li = 5.14		12.91	97.93 % - 50 cycles	3.97	[62]
Nanorods/Ni HCFIII-LMO	–	–	27.2	37.4 % - 200 cycles	1.76	[111]
rGO-LNCM	Mg/Li = 18.6	Mg/Li = 0.006	13.841	80.8 % - 30 cycles	1.4	112
Mxne-LMO	Na/Li = 16.6	–	λ/1020	94.27 % - 30 cycles		[113]
Spent $LiFePO_4$	Na/Li = 74.43	Na/Li = 0.35	14.62	60 % - 13 cycles	0.768	[114]
$LiMn_2O_4$/C/ PVDF-b-PAA	Mg/Li = 292.2	Mg/Li = 0.46	15.11	83.4 % - 20 cycles		[115]
CNT-s-LMO	Mg/Li = 60	Mg/Li = 0.17	1.6 m	90 % - 100 cycles		[116]

Note: *: recovery rate. M/Li^+: the content of impurity ions in brine; $M1/Li^+$: the content of impurity ions in the enrichment solution after multiple cycles; λ: the separation factor of Li^+ from other impurity ions.

lithium ions' intercalation and de-intercalation efficiency [118]. This is because during the electrochemical process, the transport of ions in brine is affected by diffusion and concentration polarization, and the transport impedance limits the migration rate of ions. The diffusion process involves the random movement of ions in brine, while the aggregation of ions on the electrode surface causes concentration polarization. These transport limitations reduce the insertion rate of lithium ions. Meanwhile, the structure and morphology of the electrode material also affect the accessibility of ions in brine and the exposure of active sites on the electrode surface, thereby affecting the reaction rate and lithium extraction efficiency [67]. On the other hand, carbon materials used as conductive additives usually have strong hydrophobicity, resulting in large interfacial tension. However, salt water is a high-viscosity liquid which seriously affects the full contact and wetting between salt water and active materials, directly leading to large solid-liquid interface transfer resistance and low electrochemical surface utilization efficiency. In addition, the stability of active materials also exists as a huge challenge. For example, the dissolution of Mn in the electrochemical reaction of LMO can easily destroy the structure of LMO. Therefore, material design is the key to improving lithium extraction efficiency. Typically exhibit strong hydrophobicity, which leads to high interfacial tension. Additionally, salt water is a high-viscosity liquid that significantly hinders the contact and wetting between the salt water and active materials. This results in substantial solid-liquid interface transfer resistance and reduced electrochemical surface utilization efficiency. Furthermore, the stability of active materials poses a significant challenge. For instance, the dissolution of Mn during the electrochemical reaction of LMO can easily compromise its structure. Thus, effective material design is crucial for enhancing lithium extraction efficiency.

3.1.2. Competition of impurity ions

Another reason for the low efficiency of this technology is the competition of impurity ions due to the compositional characteristics of the brine itself [80,119,120]. The intrinsic matter is that impurity ions embed in the active material and occupy the Li^+ site, reducing the Li^+ site rate [64]. Meanwhile, the Li^+ deporting process in the electrochemical method involves the chemical reaction on the electrode surface. These reactions are usually carried out with the surface active site as the active center [119]. Due to the limited active site on the electrode surface, impurity ions may participate in the chemical reaction, and only a few sites can participate in the process of Li^+ intercalation. Thus, the active site on the electrode surface limits the reaction rate. If the number of active sites is limited or the distribution of active sites is not uniform, the reaction rate will be slow.

A key challenge in effectively comparing Li^+ selectivity across different electrodes is the variation in selectivity performance metrics used in previous studies. Typically, these studies have measured selectivity by calculating the ratio of the concentration of lithium (Li) to that of another cation (M) in the recovered solution (Eq. (7)) [61].

$$K_{Li/M} = \left(C_{Li}^{T}\right)/\left(C_{M}^{S}\right) \tag{7}$$

The partition coefficient of each component can be defined as the ratio of its concentration in the recovery solution to its concentration in the source solution, i.e. for Li^+ and another ion M (Eqs. (8)–(9)).

$$K_{Li} = \left(C_{Li}^{T}\right)/\left(C_{Li}^{S}\right) \tag{8}$$

$$K_{M} = \left(C_{M}^{T}\right)/\left(C_{M}^{S}\right) \tag{9}$$

For systems in thermodynamic equilibrium between two phases, these indices typically represent the distribution coefficients of different ions. However, this simple attribution does not apply to situations where the recovery solution and the source solution are not in thermodynamic equilibrium due to the influence of various process conditions. In thermodynamic equilibrium between two phases, these indices typically represent the distribution coefficients of different ions. However, this straightforward attribution does not hold when the recovery solution and the source solution are out of thermodynamic equilibrium due to varying process conditions. Instead, we can define the separation factor

(SF) as a metric to evaluate the overall effectiveness of Li^+ enrichment in these systems (Eq. (10)) [121].

$$SF = \frac{K_{Li}}{K_M} = \frac{(C_{Li}/C_M)^r}{(C_{Li}/C_M)^s} \quad (10)$$

This quantity can be expressed as the ratio of the relative concentrations of Li^+ and contaminant ions M in the recovered solution to their relative concentrations in the source solution. Despite the electrode having a high intrinsic selectivity for Li^+, the SF magnitude in the electro-adsorption system for Li^+ recovery is primarily affected by the initial composition of the brine rather than the electrode performance. Thus, even using the same lithium capture electrode, This quantity is defined as the ratio of the relative concentrations of Li^+ and contaminant ions (M) in the recovered solution to their relative concentrations in the source solution. Despite the electrode's high intrinsic selectivity for Li^+, the magnitude of the SF in the electro-adsorption system for Li^+ recovery is primarily influenced by the initial composition of the brine rather than the performance of the electrode. Consequently, even with the same lithium capture electrode, the SF can range from 1 to as high as 5316, which complicates the comparison of effective SF values across different systems. In contrast, K_{Li}/K_M represents the quality of the final recovered solution, which is critical in determining the purity of the final lithium product. However, the specific ion types present in the recovered solution depend on the initial brine composition. Therefore, lithium purity (PLi), defined as the percentage of lithium ions in the final recovered solution, offers a more direct measure of recovery performance. Thus, PLi is suggested to be incorporated into performance evaluations and consistently reports application conditions and initial Li^+ concentrations. The ratio KLi/M serves as an indicator of the quality of the final recovered solution, which is essential for assessing the purity of the lithium product. The specific types of ions present in the recovered solution are influenced by the initial composition of the brine. Consequently, lithium purity (PLi), defined as the percentage of lithium ions in the final recovered solution, offers a more direct and relevant measure of recovery performance. Therefore, it is recommended that PLi be integrated into performance evaluations, alongside the consistent reporting of application conditions and initial concentrations of $_{Li} + _{.}121$.

3.2. Immaturity of process parameters

The development of electrochemical lithium extraction technology is relatively recent and remains in the exploratory and initial application stages [122]. Many process parameters and technical details still require optimization and validation [123]. The immaturity of the technology may result in low efficiency, high costs, and difficulty in achieving large-scale industrial applications. Key process parameters include temperature, lithium-ion concentration, current density, and voltage range [117]. Temperature directly affects the diffusion rate of lithium ions and the electrochemical reaction rate of the material. Higher temperatures can severely impact the lithium extraction capacity and stability of the active material. In addition, the adaptability of this technology to different lithium ion concentrations in brine is not clear, and the extraction efficiency may vary greatly depending on the concentration. The lack of clear adaptability limits the applicability of this process, hindering its promotion to various saline resources. Furthermore, current directly influences the electrochemical reaction rate and lithium extraction efficiency. Excessive or insufficient current can degrade the material's performance and the extraction process. Improper current control can lead to high energy consumption, material degradation, and equipment damage, affecting the process's economy and operability. Moreover, voltage is another crucial parameter driving the electrochemical reaction. Different voltage conditions can significantly impact the reaction rate and lithium-ion migration efficiency. Elevated temperatures can profoundly affect both the lithium extraction capacity and the stability of the active materials utilized in the process. Moreover, the technology's adaptability to varying concentrations of lithium ions in brine is not well established, leading to significant variations in extraction efficiency depending on the concentration levels. This lack of clear adaptability constrains the applicability of the process, thereby limiting its implementation across a range of saline resources. Additionally, the current plays a pivotal role in determining the electrochemical reaction rate and the efficiency of lithium extraction. Both excessive and insufficient current can negatively impact the material's performance and disrupt the extraction process. Inadequate control of current can result in increased energy consumption, degradation of materials, and potential damage to equipment, which ultimately affects the economic feasibility and operational reliability of the process. Furthermore, voltage is another critical parameter influencing the electrochemical reaction, with varying voltage conditions significantly affecting both the reaction rate and the efficiency of lithium-ion migration [117]. Improper voltage settings can result in poor separation, reduced electrochemical stability, and even side reactions.

3.3. Energy cost

Electrochemical methods require a large amount of energy to achieve Li^+ intercalation. This makes energy costs an important consideration, especially when using traditional energy sources such as fossil fuels, increasing environmental pollution and energy costs. Additionally, the use of supporting electrolytes (NaCl) and other chemicals in electrochemical processes increases energy costs as well as the preparation, handling, and recycling costs. Moreover, most of the brine is in the Gobi drought, a perennial lack of water and electricity [124]. Therefore, the transmission of water and electricity also increases the cost of human and material resources. Importantly, the brine may be electrolyzed in the process of lithium extraction, which consumes more energy.

The key methos to solve the energy cost is to improve current efficiency and reduce energy consumption. The expression methods for current efficiency (Eq. (11)) [125], energy efficiency (Eq. (12)), and energy consumption are introduced below [121].

Current efficiency

$$\eta(\%) = F \times \Delta c \times V1000 \times M_{Li} \times 0tI(t)dt \times 100\% \quad (11)$$

Energy efficiency

$$ESEVWhm^{-1} = U \times M_{Li} \times 0tI(t)dt \times 3.6 \times \Delta c \times V \quad (12)$$

where, F (96,485C·mol^{-1}) is Faraday's constant; the concentration difference $\triangle$c mg·L^{-1} is the concentration difference of Li^+ in the intercalated or deintercalated process; V (L) s the lithium solution (or recovery solution) volume; U (V) is the potential applied to the working electrode; M_{Li} (6.941 g·mol^{-1}) is the molar mass of lithium. I (A) and t (s) are the current and time of the intercalation (or unintercalation) process, respectively. A comprehensive consideration of current efficiency, energy consumption, and release capacity is an indicator of maximizing energy cost savings. For example, Deng et al. [54] found that the current efficiency of the electrode dropped sharply at −0.4 V, which was mainly caused by water decomposition. Thus, considering the capacity, specific energy consumption, and current efficiency, −0.8 V and 0.8 V were selected as the intercalation and unintercalation potentials, respectively. In addition, the three different expressions of energy consumption and their relationships are as follows. The energy consumption W_0 (J) of each cycle is calculated by integrating the voltage curve as follows [24,126], where $\triangle$E (V) is the battery voltage (Eq. (13)).

$$W_0 = \oint_c \triangle Edq \quad (13)$$

Energy consumption E (Wh·mol^{-1}) can be defined as the equation (Eq. (14)) [105,125].

$$E = \frac{M_{Li} \sum \int_0^t \triangle E(t) I(t) dt}{3600(c_0 v_0 - c_s v_s)} \quad (14)$$

The energy consumption W ($J \cdot mol^{-1}$ or $Wh \cdot mol^{-1}$) can also be described as the molar change in the area ratio of the cyclic charge and discharge curve, which is calculated as follows (Eq. (15)) [59,85]. Vr is the volume of the outflow solution.

$$W = \frac{\oint \triangle E dq}{(C_s - C_0) \times V_r} \quad (15)$$

The formula commonly used to calculate energy consumption is Eq. (14), which is based on Eq. (13) and includes a parameter for the molar mass parameter of lithium. Utilizing E as a metric for assessing energy consumption in ELE is particularly effective because it provides an objective measure. However, it is notable that variations in the concentrations and volumes of solutions can significantly influence the results. Therefore, to accurately compare the energy consumption of different projects, it is essential to use feed solutions and devices that are similar in their specifications.

3.4. Impact on the environment

ELE technology is primarily used for brine in plateau areas, which have fragile environments. Thus, the environmental impact of this technology poses a significant challenge [6,7,123]. The electrochemical lithium extraction process generates high-salinity wastewater. If it is directly discharged into the brine, it will inevitably reduce the quality of the brine. Increase the difficulty of lithium extraction. The definition of the required and tolerable amount of waste salt water returned to a salt lake should take into account its water balance, geotechnical aspects and biodiversity impacts. If not properly treated, the discharge of these wastewater can salinize the surrounding soil and water, damaging the ecosystem. Additionally, brine electrolysis may occur in the ELE process. Untreated brine can lead to chemical pollution and acidification in plateau areas. Furthermore, cleaning the electrodes consumes substantial water. The plateau region faces water shortages [124]. Wastewater discharge and excessive water use will exacerbate local water shortages. Moreover, the unique climatic conditions in plateau regions may worsen the diffusion and deposition of pollutants, causing more extensive and severe environmental impacts. Meanwhile, the active substance may fall off during the electrode operation and be mixed with the brine, inevitably introducing non-brine native elements to the entire brine environment. Water quality safety is affected. Therefore, addressing the environmental impact of ELE technology is crucial for achieving rapid industrialization.

4. Outlook

The efficiency of lithium extraction is determined by the material, electrolyzer and process parameters. Fig. 14 shows the outlook of lithium extraction efficiency. The extraction efficiency of lithium is mainly limited by the electrode reaction rate and the ion transfer rate. Improving the electrochemical performance of the working electrode is the key to improving the extraction efficiency of lithium. Currently, various materials have been studied and developed, such as LMO, LFP, etc. [89,127] To improve the lithium extraction capacity, cycle stability, and ion selectivity, advanced methods are used to guide the synthetic method and predict output performance, such as large language model (LLM) and density functional theory (DFT) [128]. In addition, the modification of materials is vital to optimize the lithium extraction efficiency, including element doping, coating of functional materials, etc. [88] Meanwhile, it is necessary to consider the high saline-alkali environment under lithium sources such as seawater and brine. By exploring the relationship between lattice size changes and corrosion, protective coatings can be developed to enhance the corrosion resistance and hydrophilicity of electrode materials [67,129]. Another focus is to explore new electrode materials and manufacturing technologies. This includes developing innovative synthesis strategies or using structurally enhanced materials [13].

Second, it is critical to optimize the system on a larger scale to improve the efficiency and sustainability of ELE [120,130]. This includes the design of the electrolyzer and the optimization of the process parameters. The optimization of the electrolytic cell can be started from the intercalating mode of electrodes inside the cell, the design of the electrode pile and the flow mode of brine. Furthermore, it can be considered from the aspect of mass transfer of brine to avoid the phenomenon of concentration polarization. The electrode stack can be designed to achieve balanced electrode extraction in series mode. The flow of brine can be turned to hydrodynamic considerations to increase the contact between the large area electrode and Li^+. In addition, the fixed electrode in the electrolyzer can also be changed to the flowing electrode, which will greatly improve the contact area between the active substance and the brine. However, it adopts a high-demand electrolytic cell design. Active substances in mobile electrodes are

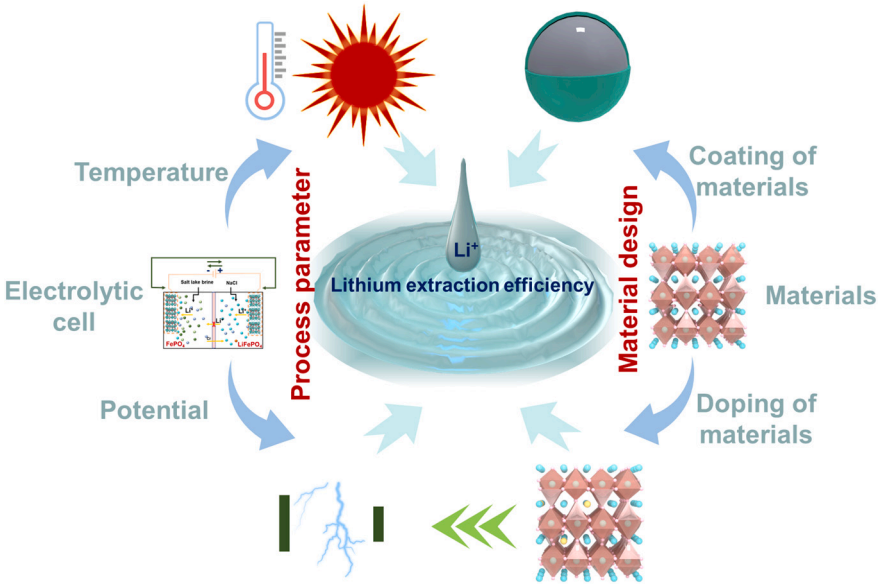

Fig. 14. A schematic of the future development of ELE technology.

difficult to recover and easily lost, causing economic problems. Solid-liquid separation can be achieved by the centrifugal principle. It can be combined with advanced AI technology to implement smart salt pans, comprehensively improve the degree of automation, and ensure the stability of the electrolytic cell. The optimization of the electrolytic cell can be systematically addressed by evaluating several critical factors, including the configuration of the electrodes, the architecture of the electrode stack, and the hydrodynamic behavior of the brine. Additionally, it is imperative to consider the mass transfer dynamics to mitigate the risk of concentration polarization. The design of the electrode stack may be tailored to ensure balanced electrode extraction in a series arrangement. Moreover, improving the hydrodynamic conditions of brine flow can enhance the interaction between the electrodes and Li^+ by increasing the effective contact area. Another viable approach involves transitioning from fixed electrodes to a flowing electrode system, which would considerably augment the interface between the active materials and the brine. However, this strategy necessitates a sophisticated design of the electrolytic cell, as the recovery of active materials from mobile electrodes poses significant challenges and may result in economic inefficiencies. Effective solid-liquid separation can be accomplished through centrifugal methods. Furthermore, the integration of advanced artificial intelligence technologies holds the potential to facilitate the development of smart salt pans, thereby enhancing automation and ensuring the operational stability of the electrolytic cell [130]. It can also be integrated with solar, wind, and energy storage technologies to reduce the consumption of electric energy and reduce costs [131–136]. Notably, most salt lakes are located at high latitudes and altitudes with a high annual average global solar radiation values of $>2000\ kWh{\cdot}m^{-2}$ [7,137]. They are the ideal places to harvest solar energy to support lithium-ion extraction.

Finally, the process parameters include the removal voltage of Li^+, the appropriate temperature and the amount of active material loaded on the electrode [117]. The competition of impurity ions can be reduced by the appropriate demounting potential. Meanwhile, the use of low current density to extract Li^+ can maximize the utilization of energy. Despite, the ion dynamics are better at high temperatures, the performance of electrode materials faces great challenges. It is also important to balance the high performance of lithium ions in electrode materials and the ion dynamics at high temperatures [138]. The loading capacity of active material is closely related to the dynamics of Li^+, which can realize the rapid transport of ion electrons from the perspective of constructing a 3D network structure and low tortuous electrode. Meanwhile, multi-technology coupling can accelerate the rapid industrialization of the industry, electrochemical lithium extraction coupled with membrane method, extraction method or ion sieve method, explore the applicability of the technology in various stages of brine, focusing on the feasibility and economy of the original brine lithium extraction technology [123]. Notably, it is vital to focus on the development of new technologies, develop comprehensive treatment of high-salt wastewater and lithium reuse technology, and promote the development of lithium extraction technology from salt lake brine to the direction of efficiency, simplicity, and environmental protection.

Through systematic research and optimization of these process parameters, the maturity of electrochemical lithium extraction technology can be gradually improved, and more efficient and economical lithium resource extraction can be achieved. These challenges and research directions will provide important guidance for future technological improvements.

5. Conclusion

To sum up, the paper reviews the progress of lithium extraction from brine by ELE technology, focusing on the influence of electrode materials and process parameters on lithium extraction efficiency. The review comprehensively introduced the development of the preparation and modification of electrode materials. The electrode material's electronic conductivity and chemical stability were improved by adjusting the structure, controlling the morphology, doping the element, and modifying the interface. The lithium extraction performance of the material is improved. In addition, larger-scale system optimization is the key to improving the efficiency and sustainability of the lithium extraction process, which includes optimizing the electrolytic cell process parameters and the design of the electrode sheet. The process parameters of the electrolytic cell can be started from the design of the electrolytic cell, the optimization of potential, and the control of the appropriate temperature. The review provides a comprehensive overview of the advancements in the preparation and modification of electrode materials. Enhancements in electronic conductivity and chemical stability are achieved through structural adjustments, morphological control, element doping, and interface modifications, thereby improving lithium extraction performance. Furthermore, optimizing larger-scale systems is crucial for enhancing the efficiency and sustainability of the lithium extraction process. This optimization encompasses the refinement of process parameters within the electrolytic cell and the design of electrode sheets. Key parameters include the electrolytic cell design, optimization of the applied potential, and maintenance of an appropriate temperature. The design of the electrode plate should pay attention to the capacity and speed of lithium extraction. As the technology progresses, it is possible to scale up by overcoming technical and economic barriers, ensuring operational reliability and stability in the industrial application.

Supplementary data to this article can be found online at https://doi.org/10.1016/j.desal.2025.118570.

CRediT authorship contribution statement

Junyi Zhang: Conceptualization, Writing – original draft, Figures edition. Tiandong Chen: Conceptualization, Writing – original draft, Figures edition. Chunxi Hai: Writing – review & editing. Yanxia Sun: Writing – review & editing. Shengde Dong: Writing – review & editing. Xin He: Writing – review & editing. Qi Xu: Writing – review & editing. Hongli Su: Conceptualization, Figures edition, Writing – review & editing. Luxiang Ma: Conceptualization, Figures edition, Writing – review & editing. Yuan Zhou: Conceptualization, Supervision, Writing – review & editing.

Declaration of competing interest

There are no conflicts to declare.

Acknowledgements

This work was supported by the National Key Research and Development Program of China (Grant No. 2021YFB2400401).

Data availability

No data was used for the research described in the article.

References

[1] B. Dunn, H. Kamath, J. Tarascon, Electrical energy storage for the grid: a battery of choices, Science 334 (6058) (2011) 928.
[2] J. Duan, X. Tang, H. Dai, Y. Yang, W. Wu, X. Wei, Y. Huang, Building safe lithium-ion batteries for electric vehicles: a review, Electrochem. Energy Rev. 3 (2020) 1.
[3] F. Maisel, C. Neef, F. Marscheider-Weidemann, N.F. Nissen, A forecast on future raw material demand and recycling potential of lithium-ion batteries in electric vehicles, Resour. Conserv. Recycl. 192 (2023) 106920.
[4] H. Yuan, M. Li, L. Cui, L. Wang, F. Cheng, Electrochemical extraction technologies of lithium: development and challenges, Desalination (2024) 118419.
[5] M. Zheng, E. Xing, X. Zhang, M. Li, D. Che, L. Bu, J. Han, C. Ye, Classification and mineralization of global lithium deposits and lithium extraction technologies for exogenetic lithium deposits, China Geol. 6 (4) (2023) 547.

[6] Y. Hu, H. Su, Z. Zhu, T. Qi, Q. Pang, Environmentally benign techniques of lithium extraction from salt lakes: a review, Environ. Chem. Lett. 22 (1) (2024) 105.
[7] M.L. Vera, W.R. Torres, C.I. Galli, A. Chagnes, V. Flexer, Environmental impact of direct lithium extraction from brines, Nat. Rev. Earth Environ. 4 (3) (2023) 149.
[8] D. Fuentealba, C. Flores-Fernández, E. Troncoso, H. Estay, Technological tendencies for lithium production from salt lake brines: Progress and research gaps to move towards more sustainable processes, Resour. Policy 83 (2023) 103572.
[9] Y. Sun, Y. Wang, Y. Liu, X. Xiang, Highly efficient lithium extraction from brine with a high sodium content by adsorption-coupled electrochemical technology, ACS Sustain. Chem. Eng. 9 (33) (2021) 11022.
[10] J. Yu, D. Fang, H. Zhang, Z.Y. Leong, J. Zhang, X. Li, H.Y. Yang, Ocean mining: a fluidic electrochemical route for lithium extraction from seawater, ACS Mater. Lett. 2 (12) (2020) 1662.
[11] W. Xu, L. He, Z. Zhao, Lithium extraction from high mg/li brine via electrochemical intercalation/deintercalation system using limn2o4 materials, Desalination 503 (2021) 114935.
[12] Z. Wang, Z. Chen, Y. Li, X. Ren, X. Xiong, Z. Lu, L. Deng, Photothermal-enhanced ion transport for efficient electrochemical lithium extraction at low temperatures, Nano Energy 131 (2024) 110249.
[13] Y. Zeng, W. Li, Z. Wan, S. Qin, Q. Huang, W. Cai, Q. Wang, M. Yao, Y. Zhang, Electrochemically mediated lithium extraction for energy and environmental sustainability, Adv. Funct. Mater. 34 (2024) 2400416.
[14] S. Kim, J.S. Kang, H. Joo, Y.-E. Sung, J. Yoon, Understanding the behaviors of λ-mno2 in electrochemical lithium recovery: key limiting factors and a route to the enhanced performance, Environ. Sci. Technol. 54 (14) (2020) 9044.
[15] H. Kanoh, K. Ooi, Y. Miyai, S. Katoh, Selective electroinsertion of lithium ions into a platinum/.lambda.-manganese dioxide electrode in the aqueous phase, Langmuir 7 (9) (1991) 1841.
[16] J. Cui, H. Xu, Y. Ding, J. Tian, X. Zhang, G. Jin, Recovery of lithium using h4mn3. 5ti1. 5o12/reduced graphene oxide/polyacrylamide composite hydrogel from brine by ads-esix process, Chin. J. Chem. Eng. 44 (2022) 20.
[17] Q. Wang, X. Du, F. Gao, F. Liu, M. Liu, X. Hao, K. Tang, G. Guan, A. Abudula, A novel h1. 6mn1. 6o4/reduced graphene oxide composite film for selective electrochemical capturing lithium ions with low concentration, Sep. Purif. Technol. 226 (2019) 59.
[18] B. Hu, B. Zhang, Y. Wang, M. Li, J. Yang, J. Liu, Prussian blue analogue derived 3d hollow licomno4 nanocube for selective extraction of lithium by pseudo-capacitive deionization, Desalination 560 (2023) 116662.
[19] J. Zhang, S. Wei, C. Zhao, S. Zia, C. Liu, T. Deng, X. Yu, Membrane-free electrochemical extraction of lithium from geothermal water with transition metal ferrocyanide as a counter electrode, Appl. Energy 373 (2024) 123956.
[20] J. Lim, H. Lee, S. Lee, S. Hong, Capacitive deionization incorporating a fluidic mof-cnt electrode for the high selective extraction of lithium, Desalination 578 (2024) 117403.
[21] W. Wang, G. Hong, Y. Zhang, X. Yang, N. Hu, J. Zhang, P. Sorokin, L. Shao, Designing an energy-efficient multi-stage selective electrodialysis process based on high-performance materials for lithium extraction, J. Membr. Sci. 675 (2023) 121534.
[22] K. Morita, T. Matsumoto, T. Hoshino, Efficient lithium extraction via electrodialysis using acid-processed lithium-adsorbing lithium lanthanum titanate, Desalination 543 (2022) 116117.
[23] D. Jiang, R. Xu, L. Bai, W. Wu, D. Luo, Z. Li, T. Asahi, Y. Mai, Z. Liu, Y. Yamauchi, et al., Insights into electrochemical paradigms for lithium extraction: Electrodialysis versus capacitive deionization, Coord. Chem. Rev. 516 (2024) 215923.
[24] M. Pasta, A. Battistel, F. La Mantia, Batteries for lithium recovery from brines, Energy Environ. Sci. 5 (11) (2012) 9487.
[25] L. Cui, Q. Zhang, C. Li, L. Wang, D. Sun, F. Cheng, Liquid membrane coupled electrodialysis system for highly-efficient lithium recovery from fly ash acid leaching solution, Chem. Eng. Process. Process Intensif. 195 (2024) 109650.
[26] Y. Ha, H.B. Jung, H. Lim, P.S. Jo, H. Yoon, C. Yoo, T.K. Pham, W. Ahn, Y. Cho, Continuous lithium extraction from aqueous solution using flow-electrode capacitive deionization, Energies 12 (15) (2019) 2913.
[27] J. Luo, W. Cui, P. He, Y. Xia, Raising the cycling stability of aqueous lithium-ion batteries by eliminating oxygen in the electrolyte, Nat. Chem. 2 (9) (2010) 760.
[28] Y. Zhang, W. Sun, R. Xu, L. Wang, H. Tang, Lithium extraction from water lithium resources through green electrochemical-battery approaches: a comprehensive review, J. Clean. Prod. 285 (2021) 124905.
[29] M.R. Mojid, K.J. Lee, J. You, A review on advances in direct lithium extraction from continental brines: ion-sieve adsorption and electrochemical methods for varied mg/li ratios, Sustain. Mater. Technol. 40 (2024) e00923.
[30] Z. Guo, Z. Ji, J. Wang, X. Guo, J. Liang, Electrochemical lithium extraction based on "rocking-chair" electrode system with high energy-efficient: the driving mode of constant current-constant voltage, Desalination 533 (2022) 115767.
[31] R.A. House, P.G. Bruce, Lightning fast conduction, Nat. Energy 5 (3) (2020) 191.
[32] X. Xu, Y. Chen, P. Wan, K. Gasem, K. Wang, T. He, H. Adidharma, M. Fan, Extraction of lithium with functionalized lithium ion-sieves, Prog. Mater. Sci. 84 (2016) 276.
[33] J.C. Hunter, Preparation of a new crystal form of manganese dioxide: λ-mno2, J. Solid State Chem. 39 (2) (1981) 142.
[34] K. Ooi, Y. Miyai, S. Katoh, H. Maeda, M. Abe, Topotactic lithium (1+) insertion to. Lambda.-manganese dioxide in the aqueous phase, Langmuir 5 (1) (1989) 150.
[35] F. Marchini, F.J. Williams, E.J. Calvo, Electrochemical impedance spectroscopy study of the lixmn2o4 interface with natural brine, J. Electroanal. Chem. 819 (2018) 428.
[36] R. Yin, Z. Zhao, W. Xu, L. He, Limn2o4 submicronization: shorten li+ diffusion pathway for enhancing electrochemical lithium extraction and cycle performance, Sep. Purif. Technol. 359 (2025) 130394.
[37] J. Gu, L. Chen, L. Fan, G. Luo, X. Li, X. Chen, H. Ji, Y. Chao, W. Zhu, Multistage regulation of limn2o4 electrode for electrochemical lithium extraction from salt-lake, Desalination (2024) 117828.
[38] X. An, Z. Du, B. Qiao, S. Wang, P. Wang, X. Ma, Y. Li, X. Du, X. Hao, G. Guan, Co-doping induced mn-vacancy limn2o4 based membrane electrode for lithium extraction by electrochemically switched ion permselective process, Desalination 591 (2024) 118016.
[39] G. Luo, M. Zhou, Y. Chao, P. Cui, X. Li, L. Chen, G. Jiang, W. Zhu, Z. Liu, C. Xu, Augmented electrochemical extraction lithium performance via interface alloying modification, Sep. Purif. Technol. 354 (2025) 128683.
[40] G. Zhou, X. Li, L. Chen, G. Luo, J. Gu, J. Zhu, J. Yu, J. Yin, Y. Chao, W. Zhu, Construction of porous disc-like lithium manganate for rapid and selective electrochemical lithium extraction from brine, Chin. J. Chem. Eng. 54 (2023) 316.
[41] J. Gu, G. Zhou, L. Chen, X. Li, G. Luo, L. Fan, Y. Chao, H. Ji, W. Zhu, Particle size control and electrochemical lithium extraction performance of limn2o4, J. Electroanal. Chem. 940 (2023) 117487.
[42] Y. Wang, X. Yang, L. Gao, Y. Wu, Y. Chen, Towards high adsorption performance and cycling stability for spinel lithium ion-sieve h1. 6mn1. 6o4 by coating li2zro3 and doping zr, Colloids Surf. A Physicochem. Eng. Asp. 638 (2022) 128283.
[43] Y. Wang, J. Zhang, Z. Cheng, X. Xiang, Hydrophilic modification using polydopamine on core–shell li1. 6mn1. 6o4@ carbon electrodes for lithium extraction from lake brine, ACS Sustain. Chem. Eng. 10 (27) (2022) 8970.
[44] G. Luo, X. Li, L. Chen, Y. Zhang, J. Gu, Y. Chao, W. Zhu, Z. Liu, C. Xu, Island-like ceo2 decorated limn2o4: surface modification enhancing electrochemical lithium extraction and cycle performance, Chem. Eng. J. 455 (2023) 140928.
[45] J. Gu, L. Chen, X. Li, G. Luo, L. Fan, Y. Chao, H. Ji, W. Zhu, Multifunctional alpo4 reconstructed limn2o4 surface for electrochemical lithium extraction from brine, J. Energy Chem. 89 (2024) 410.
[46] Z. Zhang, X. Du, Q. Wang, F. Gao, T. Jin, X. Hao, P. Ma, J. Li, G. Guan, A scalable three-dimensional porous λ-mno2/rgo/ca-alginate composite electroactive film with potential-responsive ion-pumping effect for selective recovery of lithium ions, Sep. Purif. Technol. 259 (2021) 118111.
[47] Y. Mu, C. Zhang, W. Zhang, Y. Wang, Electrochemical lithium recovery from brine with high mg2+/li+ ratio using mesoporous λ-mno2/limn2o4 modified 3d graphite felt electrodes, Desalination 511 (2021) 115112.
[48] G. Tian, J. Gao, M. Wang, X. Wen, Y. Liu, J. Xiang, L. Zhang, P. Cheng, J. Zhang, N. Tang, Structural stabilization of cr-doped spinel limn2o4 for long-term cyclability towards electrochemical lithium recovery in original brine, Electrochim. Acta 475 (2024) 143361.
[49] X. Meng, Y. Jing, J. Li, Z. Sun, Z. Wu, Electrochemical recovery of lithium from brine by highly stable truncated octahedral lini0. 05mn1. 95o4, Chem. Eng. Sci. 283 (2024) 119400.
[50] X. Zhao, H. Yang, Y. Wang, L. Yang, L. Zhu, Lithium extraction from brine by an asymmetric hybrid capacitor composed of heterostructured lithium-rich cathode and nano-bismuth anode, Sep. Purif. Technol. 274 (2021) 119078.
[51] Y. Wang, J. Zhang, Z. Cheng, X. Xiang, Hydrophilic Modification Using Polydopamine on Core–Shell $Li_{1.6}Mn_{1.6}O_4$ @Carbon Electrodes for Lithium Extraction from Lake Brine, ACS Sustain. Chem. Eng. 10 (July 2022) 8970.
[52] S. Shi, L. Liu, C. Ouyang, D.-s. Wang, Z. Wang, L. Chen, X. Huang, Enhancement of electronic conductivity of lifepo 4 by cr doping and its identification by first-principles calculations, Phys. Rev. B 68 (19) (2003) 195108.
[53] L. Wang, Y. Zhou, W. Chen, J.-L. Jiang, Z.-H. Guo, Preparation of lifepo4 composite based on dual carbon sources of phytic acid and glucose and its performance for lithium extraction from salt lake, Sep. Purif. Technol. 306 (2023) 122605.
[54] J. Zhang, W. Su, B. Yi, Y. Guo, T. Deng, X. Yu, A new strategy for the preparation of highly stable and high-capacity electrodes for green electrochemical extraction of lithium, Chem. Eng. J. 454 (2023) 140416.
[55] J. Kim, Y. Lee, S. Choi, J. Shin, H. Dinh, J.W. Choi, An electrochemical cell for selective lithium capture from seawater, Environ. Sci. Technol. 49 (16) (2015) 9415.
[56] Y. Chen, H. Zhan, Y. Qiao, Z. Qian, B. Lv, Z. Wu, Z. Liu, Facet dependent ion channel of iron phosphate for electrochemical lithium extraction, Chem. Eng. J. 477 (2023) 147136.
[57] J. Xiong, Z. Zhao, D. Liu, L. He, Direct lithium extraction from raw brine by chemical redox method with lifepo4/fepo4 materials, Sep. Purif. Technol. 290 (2022) 120789.
[58] Y. Zang, C. Ding, X. Wang, Z. Wen, C. Chen, Molybdenum-doped lithium-rich layered-structured cathode material li1. 2ni0. 2mn0. 6o2 with high specific capacity and improved rate performance, Electrochim. Acta 168 (2015) 234.
[59] X. Zhao, G. Li, M. Feng, Y. Wang, Semi-continuous electrochemical extraction of lithium from brine using cf-nmmo/ac asymmetric hybrid capacitors, Electrochim. Acta 331 (2020) 135285.
[60] M.S. Park, First-principles study of native point defects in lini 1/3 co 1/3 mn 1/3 o 2 and li 2 mno 3, Phys. Chem. Chem. Phys. 16 (31) (2014) 16798.
[61] C.P. Lawagon, G.M. Nisola, R.A.I. Cuevas, H. Kim, S. Lee, W. Chung, $Li_{1-x}Ni_{0.33}Co_{1/3}Mn_{1/3}O_2$/ag for electrochemical lithium recovery from brine, Chem. Eng. J. 348 (2018) 1000.

[62] Y. Wu, P. Shi, Y. Zhong, R. Cai, Improved performance of a ni, co-doped limn2o4 electrode for lithium extraction from brine, Energy Fuel 37 (5) (2023) 4083.
[63] J. Zhou, S. Xiang, X. Wang, D. Shin, H. Zhou, Highly selective lithium extraction from salt lake via carbon-coated lithium vanadium phosphate capacitive electrode, Chem. Eng. J. 482 (2024) 148985.
[64] J. Li, W. Fan, W. Qin, C. Ma, L. Yan, Y. Guo, M. Samadiy, U. Alimov, T. Deng, The regeneration process of fepo4 in electrochemical lithium extraction: the role of alkali ions, Chem. Eng. J. 493 (2024) 152476.
[65] X. Zhao, S. Yang, Y. Hou, H. Gao, Y. Wang, D.A. Gribble, V.G. Pol, Recent progress on key materials and technical approaches for electrochemical lithium extraction processes, Desalination 546 (2023) 116189.
[66] A. Battistel, M.S. Palagonia, D. Brogioli, F. La Mantia, R. Trócoli, Electrochemical methods for lithium recovery: a comprehensive and critical review, Adv. Mater. 32 (23) (2020) 1905440.
[67] J. Zhang, W. Pan, Y. Zhou, C. Hai, Y. Xu, Y. Zhao, Y. Sun, S. Dong, X. He, Q. Xu, et al., Biochar-enhanced three-dimensional conductive network thick electrodes for efficient lithium extraction from salt lake brines with high magnesia-lithium ratios, Chemosphere 360 (2024) 142325.
[68] W. Xu, D. Liu, X. Liu, D. Wang, L. He, Z. Zhao, Highly selective and efficient lithium extraction from brines by constructing a novel multiple-crack-porous lifepo4/fepo4 electrode, Desalination 546 (2023) 116188.
[69] G. Tan, S. Wan, J. Chen, H. Yu, Y. Yu, Reduced lattice constant in al-doped limn2o4 nanoparticles for boosted electrochemical lithium extraction, Adv. Mater. 36 (14) (2024) 2310657.
[70] Q. Zhu, X. Yu, Y. Liu, Y. Wang, P. Yang, K. Liu, Electrochemical lithium extraction with continuous flow electrodes, Desalination 574 (2024) 117250.
[71] X. Zhang, Z. Li, J. Liu, F. Xu, L. Zheng, S. De Wolf, Z. Lai, X. Lu, Solar-driven ultrafast lithium extraction from low-grade brine using microfluidics-mediated vortex in scalable electrochemical reactors, Chem. Eng. J. 454 (2023) 140074.
[72] E.N. Guyes, A.N. Shocron, A. Simanovski, P. Biesheuvel, M.E. Suss, A one-dimensional model for water desalination by flow-through electrode capacitive deionization, Desalination 415 (2017) 8.
[73] V.C.E. Romero, M. Tagliazucchi, V. Flexer, E.J. Calvo, Sustainable electrochemical extraction of lithium from natural brine for renewable energy storage, J. Electrochem. Soc. 165 (10) (2018) A2294.
[74] S. Kim, J. Lee, J.S. Kang, K. Jo, S. Kim, Y.-E. Sung, J. Yoon, Lithium recovery from brine using a λ-mno2/activated carbon hybrid supercapacitor system, Chemosphere 125 (2015) 50.
[75] S. Wang, X. Yu, X. Hu, Electrochemical lithium extraction with gas flushing of porous electrodes, Nanomaterials 13 (9) (2023) 1471.
[76] Z. Yuan, Y. Yu, L. Wei, C. Wang, X. Zhong, X. Sui, Z. Yu, D.S. Han, H. Shon, Y. Chen, Thermo-osmosis-coupled thermally regenerative electrochemical cycle for efficient lithium extraction, ACS Appl. Mater. Interfaces 13 (5) (2021) 6276.
[77] S.P. Ong, V.L. Chevrier, G. Hautier, A. Jain, C. Moore, S. Kim, X. Ma, G. Ceder, Voltage, stability and diffusion barrier differences between sodium-ion and lithium-ion intercalation materials, Energ. Environ. Sci. 4 (9) (2011) 3680.
[78] W. Xu, D. Liu, L. He, X. Liu, Z. Zhao, Study on the reaction kinetics of salt lake lithium extraction electrode by electrochemical deintercalation method, J. Chem. Eng. 72 (6) (2021) 3105.
[79] Z. Hong, Q. Zhu, Y. Liu, S. Wang, J. Wu, H. Jiang, X. Hu, K. Liu, Dependence of concentration polarization on discharge profile in electrochemical lithium extraction, Desalination 527 (2022) 115567.
[80] C. Liu, Y. Li, D. Lin, P. Hsu, B. Liu, G. Yan, T. Wu, Y. Cui, S. Chu, Lithium extraction from seawater through pulsed electrochemical intercalation, Joule 4 (7) (2020) 1459.
[81] Y. Yu, Z. Yuan, Z. Yu, C. Wang, X. Zhong, L. Wei, Y. Yao, X. Sui, D.S. Han, Y. Chen, Thermally assisted efficient electrochemical lithium extraction from simulated seawater, Water Res. 223 (2022) 118969.
[82] M. Akiyama, K. Ando, Y. Oishi, Self-diffusion of constituent ions in antifluorite-cubic lithium oxide, Solid State Ion. 3 (1981) 469.
[83] X. Zhao, Y. Zhang, Y. Wang, H. Wei, Battery-type electrode materials for sodium-ion capacitors, Batteries Supercaps 2 (11) (2019) 899.
[84] D. Kalmykov, S. Makaev, G. Golubev, I. Eremeev, V. Vasilevsky, J. Song, T. He, A. Volkov, Operation of three-stage process of lithium recovery from geothermal brine: simulation, Membranes 11 (3) (2021) 175.
[85] X. Zhao, Y. Jiao, P. Xue, M. Feng, Y. Wang, Z. Sha, Efficient lithium extraction from brine using a three-dimensional nanostructured hybrid inorganic-gel framework electrode, ACS Sustain. Chem. Eng. 8 (12) (2020) 4827.
[86] X. Zhao, Y. Gong, K. Gao, Y. Wang, H.Y. Yang, Tailored lmo@ cof composite electrodes for direct electrochemical lithium extraction from high-temperature brines, Chem. Eng. J. 474 (2023) 145975.
[87] D. Liu, S. Sun, J. Yu, A new high-efficiency process for Li^+ recovery from solutions based on $LiMn_2O_4/\lambda$-MnO_2 materials, Chem. Eng. J. 377 (2019) 119825.
[88] J. Zhang, Y. Zhou, C. Hai, H. Su, Y. Zhao, Y. Sun, S. Dong, X. He, Q. Xu, T. Chen, et al., Enhancing lithium extraction efficiency from salt lake brines through three-dimensional conductive network-incorporated thick electrodes, Sep. Purif. Technol. 334 (2024) 126010.
[89] J. Zhang, Y. Zhou, C. Hai, Y. Gao, Y. Zhao, Y. Sun, S. Dong, X. He, Q. Xu, J. Chen, et al., Constructing the 3d-conductive network-incorporated thick electrodes via melamine foam for lithium extraction, Desalination 579 (2024) 117457.
[90] F. Marchini, E.J. Calvo, F.J. Williams, Effect of the electrode potential on the surface composition and crystal structure of limn2o4 in aqueous solutions, Electrochim. Acta 269 (2018) 706.
[91] Z. Guo, Z. Ji, H. Chen, J. Liu, Y. Zhao, F. Li, J. Yuan, Effect of impurity ions in the electrosorption lithium extraction process: generation and restriction of "selective concentration polarization", ACS Sustain. Chem. Eng. 8 (31) (2020) 11834.
[92] P. Jiang, L. Chen, H. Shao, S. Huang, Q. Wang, Y. Su, X. Yan, X. Liang, J. Zhang, J. Feng, et al., Methylsulfonylmethane-based deep eutectic solvent as a new type of green electrolyte for a high-energy-density aqueous lithium-ion battery, ACS Energy Lett. 4 (6) (2019) 1419.
[93] F. Wang, Y. Lin, L. Suo, X. Fan, T. Gao, C. Yang, F. Han, Y. Qi, K. Xu, C. Wang, Stabilizing high voltage licoo 2 cathode in aqueous electrolyte with interphase-forming additive, Energ. Environ. Sci. 9 (12) (2016) 3666.
[94] X. Ren, S. Chen, H. Lee, D. Mei, M.H. Engelhard, S.D. Burton, W. Zhao, J. Zheng, Q. Li, M.S. Ding, et al., Localized high-concentration sulfone electrolytes for high-efficiency lithium-metal batteries, Chem 4 (8) (2018) 1877.
[95] H. Moon, R. Tatara, T. Mandai, K. Ueno, K. Yoshida, N. Tachikawa, T. Yasuda, K. Dokko, M. Watanabe, Mechanism of li ion desolvation at the interface of graphite electrode and glyme–li salt solvate ionic liquids, J. Phys. Chem. C 118 (35) (2014) 20246.
[96] B.S. Lalia, A. Khalil, R. Hashaikeh, Selective electrochemical separation and recovery of calcium and magnesium from brine, Sep. Purif. Technol. 264 (2021) 118416.
[97] K. Ju, D. Liu, Z. Zhao, L. He, W. Xu, Efficiently separating li+ and mg2+ from brine and directly preparing li3po4 by a combination of electrochemical intercalation/deintercalation and mgnh4po4 precipitation, Sep. Purif. Technol. 324 (2023) 124643.
[98] Y. Liu, Y. Deng, Q. Zhang, H. Liu, Overview of recent developments of resource recovery from wastewater via electrochemistry-based technologies, Sci. Total Environ. 757 (2021) 143901.
[99] R. Xu, X. Xiao, G. Zhang, Y. Ye, P. Zhang, Y. Yang, S.B. Shuchi, Y. Cui, Continuous lithium extraction from brine by efficient redox-couple electrodialysis, Matter 7 (2024) 1.
[100] C. Jiang, B. Chen, Z. Xu, X. Li, Y. Wang, L. Ge, T. Xu, Ion-"distillation" for isolating lithium from lake brine, AICHE J. 68 (6) (2022) e17710.
[101] Y. Zhao, H. Wang, Y. Li, M. Wang, X. Xiang, An integrated membrane process for preparation of lithium hydroxide from high mg/li ratio salt lake brine, Desalination 493 (2020) 114620.
[102] M. Gulied, S. Zavahir, T. Elmakki, H. Park, G.H. Gago, H.K. Shon, D.S. Han, Efficient lithium recovery from simulated brine using a hybrid system: direct contact membrane distillation (dcmd) and electrically switched ion exchange (esix), Desalination 572 (2024) 117127.
[103] D. Liu, Z. Zhao, W. Xu, J. Xiong, L. He, A closed-loop process for selective lithium recovery from brines via electrochemical and precipitation, Desalination 519 (2021) 115302.
[104] L. He, W. Xu, Y. Song, Y. Luo, X. Liu, Z. Zhao, New insights into the application of lithium-ion battery materials: selective extraction of lithium from brines via a rocking-chair lithium-ion battery system, Global Chall. 2 (2) (2018) 1700079.
[105] D. Liu, W. Xu, J. Xiong, L. He, Z. Zhao, Electrochemical system with limn2o4 porous electrode for lithium recovery and its kinetics, Sep. Purif. Technol. 270 (2021) 118809.
[106] J. Xiong, L. He, Z. Zhao, Lithium extraction from high-sodium raw brine with li0. 3fepo4 electrode, Desalination 535 (2022) 115822.
[107] J. Xiong, L. He, D. Liu, W. Xu, Z. Zhao, Olivine-fepo4 preparation for lithium extraction from brines via electrochemical de-intercalation/intercalation method, Desalination 520 (2021) 115326.
[108] G. Zhou, L. Chen, X. Li, G. Luo, Z. Yu, J. Yin, L. Fan, Y. Chao, L. Jiang, W. Zhu, Construction of truncated-octahedral limn2o4 for battery-like electrochemical lithium recovery from brine, Green Energy Environ. 8 (4) (2023) 1081.
[109] X. Du, G. Guan, X. Li, A.D. Jagadale, X. Ma, Z. Wang, X. Hao, A. Abudula, A novel electroactive λ-mno 2/ppy/pss core–shell nanorod coated electrode for selective recovery of lithium ions at low concentration, J. Mater. Chem. A 4 (36) (2016) 13989.
[110] K. Sun, M. Tebyetekerwa, X. Zeng, Z. Wang, T.T. Duignan, X. Zhang, Understanding the electrochemical extraction of lithium from ultradilute solutions, Environ. Sci. Technol. 58 (8) (2024) 3997.
[111] N. Xie, Y. Li, Y. Lu, J. Gong, X. Hu, Electrochemically controlled reversible lithium capture and release enabled by limn2o4 nanorods, ChemElectroChem 7 (1) (2020) 105.
[112] X. Zhao, M. Feng, Y. Jiao, Y. Zhang, Y. Wang, Z. Sha, Lithium extraction from brine in an ionic selective desalination battery, Desalination 481 (2020) 114360.
[113] X. Zhao, L. Zheng, Y. Hou, Y. Wang, L. Zhu, Pulsed electric field controlled lithium extraction process by lmo/mxene composite electrode from brines, Chem. Eng. J. 450 (2022) 138454.
[114] M. Du, J. Guo, S. Zheng, Y. Liu, J. Yang, K. Zhang, Z. Gu, X. Wang, X. Wu, Direct reuse of lifepo4 cathode materials from spent lithium-ion batteries: extracting li from brine, Chin. Chem. Lett. 34 (6) (2023) 107706.
[115] Z. Zhang, J. Zhang, Z. Zhang, X. Du, X. Hao, X. An, G. Guan, J. Li, Z. Liu, Cross-linked pvdf-b-paa composite binder enhanced limn2o4/c film based electrode for selective extraction of lithium from brine with a high mg/li ratio, Sep. Purif. Technol. 316 (2023) 123777.
[116] X. Shang, J. Liu, B. Hu, P. Nie, J. Yang, B. Zhang, Y. Wang, F. Zhan, J. Qiu, Cnt-strung limn2o4 for lithium extraction with high selectivity and stability, Small Methods 6 (7) (2022) 2200508.
[117] K. Shinmura, K. Sasaki, E. Niwa, S. Honda, H. Tazoe, Voltage effects on lithium extraction/recovery via electrochemical pumping using a la0. 57li0. 29tio3 electrolyte, Sustain. Mater. Technol. 39 (2024) e00779.
[118] Z. Zhang, P. Luo, Y. Zhang, Y. Wang, L. Liao, B. Yu, M. Wang, J. Chen, B. Guo, X. Li, Effects of conductive agent type on lithium extraction from salt lake brine with lifepo4 electrodes, Int. J. Miner. Metall. Mater. 31 (4) (2024) 678.
[119] H. Li, L. Li, W. Li, Lithium extraction from salt lake brine with high mass ratio of mg/li using tbp-dibk extraction system, Separations 10 (1) (2022) 24.

[120] T. Ding, M. Zheng, S. Peng, Y. Lin, X. Zhang, M. Li, Lithium extraction from salt lakes with different hydrochemical types in the Tibet plateau, Geosci. Front. 14 (1) (2023) 101485.
[121] R. Trócoli, A. Battistel, F.L. Mantia, Selectivity of a lithium-recovery process based on LiFePO4, Chem. - Eur. J. 20 (32) (2014) 9888.
[122] C. Jiang, Y. Wang, Q. Wang, H. Feng, T. Xu, Production of lithium hydroxide from lake brines through electro–electrodialysis with bipolar membranes (eedbm), Ind. Eng. Chem. Res. 53 (14) (2014) 6103.
[123] J.F. Song, L.D. Nghiem, X.-M. Li, T. He, Lithium extraction from chinese salt-lake brines: opportunities, challenges, and future outlook, Environ. Sci.: Water Res. Technol. 3 (4) (2017) 593.
[124] Z. Zhang, Y. Shan, D. Zhao, M.R. Tillotson, B. Cai, X. Li, H. Zheng, C. Zhao, D. Guan, J. Liu, et al., City level water withdrawal and scarcity accounts of China, Sci. data 11 (1) (2024) 449.
[125] M. Zhao, Z. Ji, Y. Zhang, Z. Guo, Y. Zhao, J. Liu, J. Yuan, Study on lithium extraction from brines based on limn2o4/li1-xmn2o4 by electrochemical method, Electrochim. Acta 252 (2017) 350.
[126] L.L. Missoni, F. Marchini, M. del Pozo, E.J. Calvo, A limn2o4-polypyrrole system for the extraction of licl from natural brine, J. Electrochem. Soc. 163 (9) (2016) A1898.
[127] F. Marchini, D. Rubi, M. del Pozo, F.J. Williams, E.J. Calvo, Surface chemistry and lithium-ion exchange in limn2o4 for the electrochemical selective extraction of licl from natural salt lake brines, J. Phys. Chem. C 120 (29) (2016) 15875.
[128] Q. Sun, H. Chen, J. Yu, A dft investigation of the lithium extraction process under different diluent environments, Chem. Eng. Sci. 277 (2023) 118857.
[129] A. Trentin, A. Pakseresht, A. Duran, Y. Castro, D. Galusek, Electrochemical characterization of polymeric coatings for corrosion protection: a review of advances and perspectives, Polymers 14 (12) (2022) 2306.
[130] J. Zhang, Z. Cheng, X. Qin, X. Gao, M. Wang, X. Xiang, Recent advances in lithium extraction from salt lake brine using coupled and tandem technologies, Desalination 547 (2023) 116225.
[131] S. Zhang, X. Wei, X. Cao, M. Peng, M. Wang, L. Jiang, J. Jin, Solar-driven membrane separation for direct lithium extraction from artificial salt-lake brine, Nat. Commun. 15 (1) (2024) 238.
[132] H. Su, A. Nilghaz, D. Liu, L. Dai, J. Tian, J.M. Razal, K. Tang, J. Li, Harnessing the power of water: a review of hydroelectric nanogenerators, Nano Energy 116 (2023) 108819.
[133] Y. Bu, X. Li, W. Lei, H. Su, H. Yang, W. Xu, J. Li, Bioinspired topological design with unidirectional water transfer for efficient atmospheric water harvesting, J. Mater. Chem. A 11 (28) (2023) 15147.
[134] H. Su, A. Nilghaz, D. Liu, L. Dai, B. Tang, Z. Wang, J.M. Razal, J. Tian, J. Li, Self-operating seawater-driven electricity nanogenerator for continuous energy generation and storage, Chem. Eng. J. Adv. 14 (2023) 100498.
[135] H. Su, K.A.S. Usman, A. Nilghaz, Y. Bu, K. Tang, L. Dai, D. Liu, J.M. Razal, W. Lei, J. Tian, et al., Efficient energy generation from a sweat-powered, wearable, mxene-based hydroelectric nanogenerator, Device 2 (5) (2024) 100356.
[136] H. Su, A. Nilghaz, K. Tang, D. Liu, S. Zhao, J. Tian, Y. Bu, J. Li, Insights into hydroelectric nanogenerators: numerical simulation and experimental verification, J. Mater. Chem. A 12 (36) (2024) 24409.
[137] N. Sarmiento, S. Belmonte, P. Dellicompagni, J. Franco, K. Escalante, J. Sarmiento, A solar irradiation gis as decision support tool for the province of Salta, argentina, Renew. Energy 132 (2019) 68.
[138] A. Hormati, B. Rezai, H.H. Shoormasti, G.R. Paydar, Extraction of lithium ions from salt lake brine using magnetic ionic liquid: kinetic and equilibrium studies, Inorg. Chem. Commun. 142 (2022) 109693.